

Rhodium(I) and Iridium(I) Complexes with Bidentate Phosphine–Pyrazolyl Ligands: Highly Efficient Catalysts for the Hydroamination Reaction

Leslie D. Field,[†] Barbara A. Messerle,^{*,†} Khuong Q. Vuong,[†] Peter Turner,[‡] and Tim Failes[‡]

School of Chemistry, University of New South Wales, Kensington, Sydney, NSW 2052, Australia, and Crystal Structure Analysis Facility, School of Chemistry, University of Sydney, Camperdown, Sydney, NSW 2006, Australia

Received January 18, 2007

A range of rhodium(I) and iridium(I) complexes containing bidentate phosphine–pyrazolyl ligands of general formulas $[M(R_2PyP)(COD)]BPh_4$ ($R = Me, iPr, Ph, M = Ir, \mathbf{3b}–\mathbf{3d}$ and $M = Rh, \mathbf{4b}–\mathbf{4d}$), $[Ir(R_2PyP)(CO)_2]BPh_4$ ($R = Me, iPr, \mathbf{5b}, \mathbf{5c}$), and $[M(R_2PyP)(CO)Cl]$ ($R = Me, iPr, Ph, M = Ir, \mathbf{6b}–\mathbf{6d}$ and $M = Rh, \mathbf{7b}–\mathbf{7d}$) were successfully synthesized. A number of these complexes and their analogues with unsubstituted ligands are extremely active as catalysts for the intramolecular hydroamination of alkynes. The air-stable cationic iridium complexes containing 1,5-cyclooctadiene, COD, as co-ligands, $[Ir(R_2PyP)(COD)]BPh_4$ ($R = H, Me, iPr, \text{ and } Ph, \mathbf{3a}–\mathbf{3d}$), are efficient as catalysts for the cyclization of 4-pentyn-1-amine (**8**) to 2-methyl-1-pyrroline (**9**) with the turnover rate at 50% conversion (N_t) of up to 3100 h^{-1} , at $60 \text{ }^\circ\text{C}$. The cationic iridium complexes containing carbonyl co-ligands, $[Ir(R_2PyP)(CO)_2]BPh_4$ ($R = H, Me, iPr, \mathbf{5a}–\mathbf{5c}$), are moderately effective in catalyzing this reaction, and the neutral complexes $[M(R_2PyP)(CO)Cl]$ ($M = Ir, \mathbf{6a}$ Ir, **7a**) are ineffective. Generally, an increase in steric bulk of the substituent R near the nitrogen donor leads to an improvement in catalytic performance of the resulting metal complexes.

Introduction

Complexes containing hemilabile ligands have been used successfully in a range of catalytic reactions, primarily due to the ability of hemilabile ligands to liberate vacant coordination sites as well as to stabilize reactive transition metal centers during a catalytic cycle.¹ A large number of metal complexes containing potentially hemilabile hybrid bidentate P–N donor ligands have been reported.^{1–3} These studies have mainly focused on cases where the nitrogen donors are the sp^2 -N atom from pyridines^{4,5} or oxazolines^{6,7} and the P-donors are phosphines. Many late transition metal complexes (e.g., Ru, Rh, Pd, Ir) with mixed donor sp^2 -N–P ligands are efficient catalysts for a range of organic transformations including allylic substitutions,^{2,3,5} hydrogenation,^{3,6,8–10} transfer hydrogenation,^{4,10} and

hydroboration.^{3–5,11} The chemistry of metal complexes with bidentate ligands with mixed pyrazolyl–phosphine metal donors has been, however, underexplored.^{12–18} Examples of the application of pyrazolyl–phosphine donor ligands in homogeneous catalysis include palladium-catalyzed hydration of terminal alkynes,¹⁹ hydrosilylation of norbornene,²⁰ allylic amination,^{14,21} Suzuki reactions,²² nickel-promoted polymerization,²³ and rhodium-catalyzed hydroboration.^{15,24}

The hydroamination reaction of C–C double and triple bonds has been of great interest academically and in industry due to the central importance of amines and imines in organic chemistry,^{25–28} Lanthanide^{29,30} and both early^{31,32} and late transition metal^{33–38} complexes have been found to catalyze the

* Corresponding author. E-mail: b.messerle@unsw.edu.au. Fax: (+612) 93856141.

[†] University of New South Wales.

[‡] University of Sydney.

(1) Slone, C. S.; Weinberger, D. A.; Mirkin, C. A. *Prog. Inorg. Chem.* **1999**, *48*, 233–350.

(2) Gavrillov, K. N.; Polosukhin, A. I. *Russ. Chem. Rev.* **2000**, *69*, 721–743.

(3) Guiry, P. J.; Saunders, C. P. *Adv. Synth. Catal.* **2004**, *346*, 497–537.

(4) Espinet, P.; Soulantica, K. *Coord. Chem. Rev.* **1999**, *195*, 499–556.

(5) Chelucci, G.; Orrù, G.; Pinna, G. A. *Tetrahedron* **2003**, *59*, 9471–9515.

(6) Helmchen, G.; Pfaltz, A. *Acc. Chem. Res.* **2000**, *33*, 336–345.

(7) Braunstein, P.; Naud, F. *Angew. Chem., Int. Ed.* **2001**, *40*, 680–699.

(8) McIntyre, S.; Hörmann, E.; Menges, F.; Smidt, S. P.; Pfaltz, A. *Adv. Synth. Catal.* **2005**, *347*, 282–288.

(9) Pfaltz, A.; Blankenstein, J.; Hilgraf, R.; Hörmann, E.; McIntyre, S.; Menges, F.; Schönleber, M.; Smidt, S. P.; Wüstenberg, B.; Zimmermann, N. *Adv. Synth. Catal.* **2003**, *345*, 33–43.

(10) Blaser, H. U.; Malan, C.; Pugin, B.; Spindler, F.; Steiner, H.; Studer, M. *Adv. Synth. Catal.* **2003**, *345*, 103–151.

(11) Carroll, A. M.; O'Sullivan, T. P.; Guiry, P. J. *Adv. Synth. Catal.* **2005**, *347*, 609–631.

(12) Grotjahn, D. B.; Combs, D.; Van, S.; Aguirre, G.; Ortega, F. *Inorg. Chem.* **2000**, *39*, 2080–2086.

(13) Tanaka, S.; Dubs, C.; Inagaki, A.; Akita, M. *Organometallics* **2005**, *24*, 163–184.

(14) Togni, A.; Burckhardt, U.; Gramlich, V.; Pregosin, P. S.; Salzmann, R. *J. Am. Chem. Soc.* **1996**, *118*, 1031–1037.

(15) Schnyder, A.; Togni, A.; Wiesli, U. *Organometallics* **1997**, *16*, 255–260.

(16) Caiazza, A.; Dalili, S.; Yudin, A. K. *Org. Lett.* **2002**, *4*, 2597–2600.

(17) Esquiùs, G.; Pons, J.; Yáñez, R.; Ros, J.; Mathieu, R.; Donnadieu, B.; Lukan, N. *Eur. J. Inorg. Chem.* **2002**, 2999–3006.

(18) Esquiùs, G.; Pons, J.; Yáñez, R.; Ros, J.; Mathieu, R.; Lukan, N.; Donnadieu, B. *J. Organomet. Chem.* **2003**, *667*, 126–134.

(19) Grotjahn, D. B. U.S. Pat. Appl. Publ. (San Diego State University Foundation), US2002115860, 2002.

(20) Pioda, G.; Togni, A. *Tetrahedron: Asymmetry* **1998**, *9*, 3903–3910.

(21) Burckhardt, U.; Baumann, M.; Trabesinger, G.; Gramlich, V.; Togni, A. *Organometallics* **1997**, *16*, 5252–5259.

(22) Mukherjee, A.; Sarkar, A. *Tetrahedron Lett.* **2004**, *45*, 9525–9528.

(23) Mukherjee, A.; Subramanyam, U.; Puranik, V. G.; Mohandas, T. P.; Sarkar, A. *Eur. J. Inorg. Chem.* **2005**, 1254–1263.

(24) Schnyder, A.; Hintermann, L.; Togni, A. *Angew. Chem., Int. Ed. Engl.* **1995**, *34*, 931–933.

hydroamination reactions of alkynes and alkenes. Organometallic complexes with late transition metals offer the advantage of being much less oxophilic when compared with lanthanide and early transition metal complexes. Hydroamination catalysts based on late transition metals are generally the most functional group tolerant catalysts and do not normally require stringent anaerobic conditions during the catalytic process.^{25–27}

The intramolecular reaction leading to nitrogen-containing heterocyclic products is a significant target since these heterocycles are present in many biologically active compounds. The intramolecular hydroamination of alkynes is more facile than the equivalent reaction with allenes or alkenes and has been achieved by a range of catalytic systems.^{25,27} Among the late transition metal catalysts used for the intramolecular hydroamination of alkynes, palladium is now the most widely used metal, particularly in the construction of the aromatic indole nucleus.^{27,39–41} The intramolecular hydroamination of aliphatic amino-alkynes using palladium complexes as catalysts presents different challenges and is less extensively studied.^{34,40–43} The use of other late transition metal complexes as catalysts for the intramolecular hydroamination of alkynes has received increased attention recently with the focus mainly on second- and third-row metals of groups VIII, X, and XI.^{35,37,42} A few examples of using platinum,⁴⁴ silver,⁴⁵ and gold⁴⁶ complexes as catalysts for the intramolecular hydroamination of alkynes have also been reported.

Rhodium and iridium complexes have not been extensively studied for the intramolecular hydroamination of alkynes, and the development of highly efficient group IX catalysts for hydroamination remains an important goal.^{27,35,47} In our work

(25) Brunet, J. J.; Neibecker, D. In *Catalytic Heterofunctionalization*; Togni, A., Grützmacher, H., Eds.; Wiley-VCH: Weinheim, 2001; pp 91–141, and references therein.

(26) Müller, T. E.; Beller, M. *Chem. Rev.* **1998**, *98*, 675–703, and references therein.

(27) Alonso, F.; Beletskaya, I. P.; Yus, M. *Chem. Rev.* **2004**, *104*, 3079–3159, and references therein.

(28) Hultsch, K. C. *Adv. Synth. Catal.* **2005**, *347*, 367–391, and references therein.

(29) Hong, S.; Marks, T. J. *Acc. Chem. Res.* **2004**, *37*, 673–686, and references therein.

(30) Molander, G. A.; Romero, J. A. C. *Chem. Rev.* **2002**, *102*, 2161–2185.

(31) Pohlki, F.; Doye, S. *Chem. Soc. Rev.* **2003**, *32*, 104–114, and references therein.

(32) Odom, A. L. *Dalton Trans.* **2005**, 225–233, and references therein.

(33) Hartwig, J. F. *Pure Appl. Chem.* **2004**, *76*, 507–516.

(34) Lutete, L. M.; Kadota, I.; Yamamoto, Y. *J. Am. Chem. Soc.* **2004**, *126*, 1622–1623.

(35) Müller, T. E.; Pleier, A.-K. *J. Chem. Soc., Dalton Trans.* **1999**, 583–587.

(36) Hartung, C. G.; Tillack, A.; Trauthwein, H.; Beller, M. *J. Org. Chem.* **2001**, *66*, 6339–6343.

(37) Kondo, T.; Okada, T.; Suzuki, T.; Mitsudo, T. *J. Organomet. Chem.* **2001**, *622*, 149–154.

(38) Brunet, J. J.; Cadena, M.; Chu, N. C.; Diallo, O.; Jacob, K.; Mothes, E. *Organometallics* **2004**, *23*, 1264–1268.

(39) Wolfe, J. P.; Thomas, J. S. *Curr. Org. Chem.* **2005**, *9*, 625–655.

(40) Cacchi, S.; Fabrizi, G. *Chem. Rev.* **2005**, *105*, 2873–2920.

(41) Nakamura, I.; Yamamoto, Y. *Chem. Rev.* **2004**, *104*, 2127–2198, and references therein.

(42) Müller, T. E.; Grosche, M.; Herdtweck, E.; Pleier, A. K.; Walter, E.; Yan, Y.-K. *Organometallics* **2000**, *19*, 170–183.

(43) Richmond, M. K.; Scott, S. L.; Alper, H. *J. Am. Chem. Soc.* **2001**, *123*, 10521–10525.

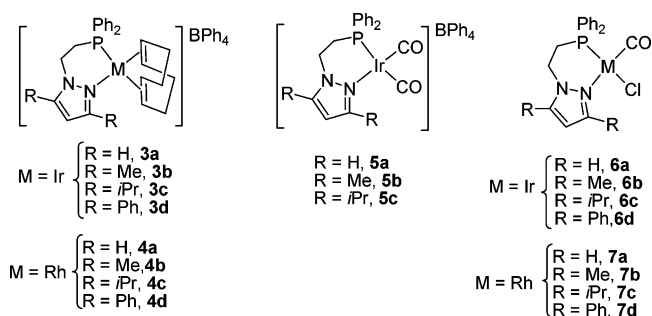
(44) Krogstad, D. A.; Owens, S. B.; Halfen, J. A.; Young, V. G., Jr. *Inorg. Chem. Commun.* **2005**, *8*, 65–69.

(45) van Esseveldt, B. C. J.; Vervoort, P. W. H.; van Delft, F. L.; Rutjes, F. P. J. T. *J. Org. Chem.* **2005**, *70*, 1791–1795.

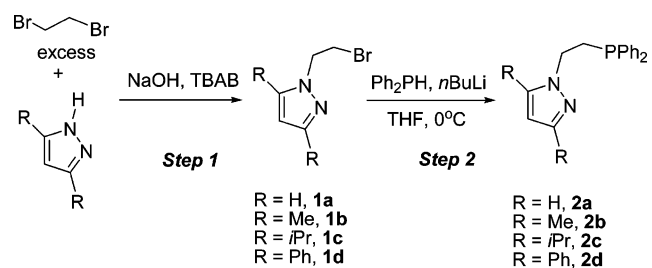
(46) Hoffmann-Röder, A.; Krause, N. *Org. Biomol. Chem.* **2005**, *3*, 387–391.

(47) Penzien, J.; Su, R. Q.; Müller, T. E. *J. Mol. Catal. A: Chem.* **2002**, *182*, 489–498.

Chart 1



Scheme 1



on hydroamination, we have reported that rhodium and iridium complexes containing bidentate bis-pyrazolyl, bis-imidazolyl, bis-*N*-heterocyclic carbene (NHC), or mixed phosphine–NHC donor ligands^{48–52} are effective catalysts for the intramolecular hydroamination of aliphatic and aromatic alkynes, and the efficiency of the catalyst changes significantly even with a small change in the ligand donor set.^{49,53,54} We have also previously reported the synthesis of rhodium and iridium complexes containing the unsubstituted bidentate phosphine–pyrazolyl donor ligand 1-[(2-diphenylphosphinoethyl)]pyrazole, PyP, and their applications as catalysts for the hydrothiolation⁵⁵ and double-hydroalkoxylation⁵⁶ of alkynes.⁵⁴ In this paper, we report the synthesis of a range of rhodium and iridium complexes containing modified phosphine–pyrazolyl donor ligands with systematic variations of substituents on the 3 and 5 positions of the pyrazolyl ring (Chart 1). The efficiency of metal complexes containing the R₂PyP (R = H, Me, *i*Pr, and Ph; **2a–2d**) ligands as catalysts for the cyclization of 4-pentyn-1-amine (**8**) to 2-methyl-1-pyrroline (**9**) is explored, and some extremely efficient catalysts are identified.

Results and Discussion

Synthesis of Phosphine–Pyrazolyl Ligands. The bidentate phosphine–pyrazolyl ligands R₂PyP (Me, **2b**; *i*Pr, **2c**; Ph, **2d**) were synthesized using a two-step sequence (Scheme 1) analogous to that used in the synthesis of 1-[(2-diphenylphosphinoethyl)]pyrazole, PyP, **2a**.⁵⁵ The first step involved the

(48) Field, L. D.; Messerle, B. A.; Vuong, K. Q.; Turner, P. *Organometallics* **2005**, *24*, 4241–4250.

(49) Burling, S.; Field, L. D.; Messerle, B. A.; Turner, P. *Organometallics* **2004**, *23*, 1714–1721.

(50) Burling, S.; Field, L. D.; Li, H. L.; Messerle, B. A.; Shasha, A. *Aust. J. Chem.* **2004**, *57*, 677–680.

(51) Burling, S.; Field, L. D.; Li, H. L.; Messerle, B. A.; Turner, P. *Eur. J. Inorg. Chem.* **2003**, 3179–3184.

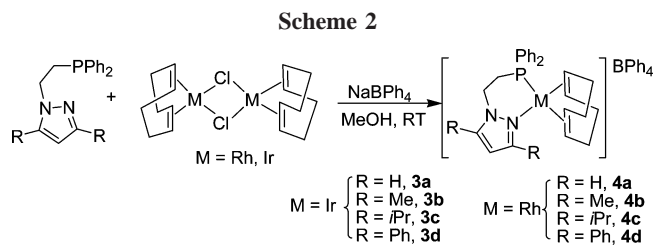
(52) Burling, S.; Field, L. D.; Messerle, B. A. *Organometallics* **2000**, *19*, 87–90.

(53) Burling, S. Ph.D. Thesis, University of Sydney, 2001.

(54) Vuong, K. Q. Ph.D. Thesis, University of New South Wales, 2006.

(55) Burling, S.; Field, L. D.; Messerle, B. A.; Vuong, K. Q.; Turner, P. *Dalton Trans.* **2003**, 4181–4191.

(56) Messerle, B. A.; Vuong, K. Q. *Pure Appl. Chem.* **2006**, *78*, 385–390.



formation of the bromo intermediates (**1a–1d**) in a biphasic reaction between the appropriate pyrazole, sodium hydroxide, and 1,2-dibromoethane (1,2-DBE) with tetrabutylammonium bromide (TBAB) as the phase transfer catalyst.⁵⁷ As the steric bulk of the R groups increased, higher temperatures were required for the reaction to proceed. Small quantities of bis(pyrazolyl)ethane ((3,5-*R*₂PyCH₂)₂, where R = H, Me, and *i*Pr) were also formed.⁵⁷ The yield of the bis(pyrazolyl)ethane byproduct increased for R = H < Me < *i*Pr, but none of the bis(pyrazolyl)ethane byproduct was observed in the reaction of 3,5-diphenylpyrazole.

In step 2 of Scheme 1, nucleophilic substitution of the bromide with the diphenylphosphide afforded the final product R₂PyP as an oxygen-sensitive viscous oil (R = Me, **2b**; *i*Pr, **2c**) or waxy solid (R = H, **2a**; Ph, **2d**) in approximately 80% yield. The ³¹P{¹H} NMR (C₆D₆) spectra of the final products show a singlet in the region –20 to –22 ppm, which is typical for alkyldiarylphosphines.⁵⁸

Synthesis of Cationic Iridium and Rhodium Complexes with R₂PyP and 1,5-Cyclooctadiene as Co-ligands, [M(R₂PyP)(COD)]BPh₄ (M = Rh, Ir). Cationic metal complexes of the general formula [M(R₂PyP)(COD)]BPh₄ (R = H, Me, *i*Pr, Ph, M = Ir, **3a–3d** and M = Rh, **4a–4d**) were synthesized by the addition of a methanol solution of the ligand to a methanol suspension/solution of the [M(μ-Cl)(COD)]₂ (M = Rh, Ir) metal precursor at room temperature (Scheme 2). Sodium tetraphenylborate was added to precipitate the metal complex. While other solvents, e.g., tetrahydrofuran, could also be used in the synthesis of these metal complexes,⁵⁵ methanol is more convenient due to the lower solubility of the product and the ease with which the sodium chloride byproduct can be washed away. All of the metal complexes were isolated in good to excellent yields. The color of all of the rhodium complexes is bright yellow, and the color of all of the iridium analogues is bright orange. The metal complexes **3a–4d** are all reasonably air stable, so that samples in the solid state can be handled in air with no apparent decomposition.

Multinuclear (¹H, ¹³C, and ³¹P) and two-dimensional (COSY, NOESY, ¹H–¹³C HMQC, and, in some cases, ¹H–¹³C HMBC) NMR spectroscopy was used to establish the solution structures of the metal complexes **3a–4d**. In many cases, the complexes are fluxional at room temperature and it was necessary to obtain the NMR spectra at low temperature to slow the chemical exchange. The chemical shifts and ¹J_{Rh–P} coupling constants are similar to those reported for other similar rhodium^{15,17} and iridium^{59–61} complexes with bidentate P–N ligands where six-membered metallacycles are formed upon chelation.

(57) López, P.; Seipelt, C. G.; Merklung, P.; Sturz, L.; Álvarez, J.; Dölle, A.; Zeidler, M. D.; Cerdán, S.; Ballesteros, P. *Bioorg. Med. Chem.* **1999**, *7*, 517–527.

(58) Davies, J. A.; Mierzwiak, J. G.; Syed, R. *J. Coord. Chem.* **1988**, *17*, 25–43.

(59) Hou, D. R.; Reibenspies, J.; Colacot, T. J.; Burgess, K. *Chem. Eur. J.* **2001**, *7*, 5391–5400.

(60) Lightfoot, A.; Schnider, P.; Pfaltz, A. *Angew. Chem., Int. Ed.* **1998**, *37*, 2897–2899.

(61) Menges, F.; Neuburger, M.; Pfaltz, A. *Org. Lett.* **2002**, *4*, 4713–4716.

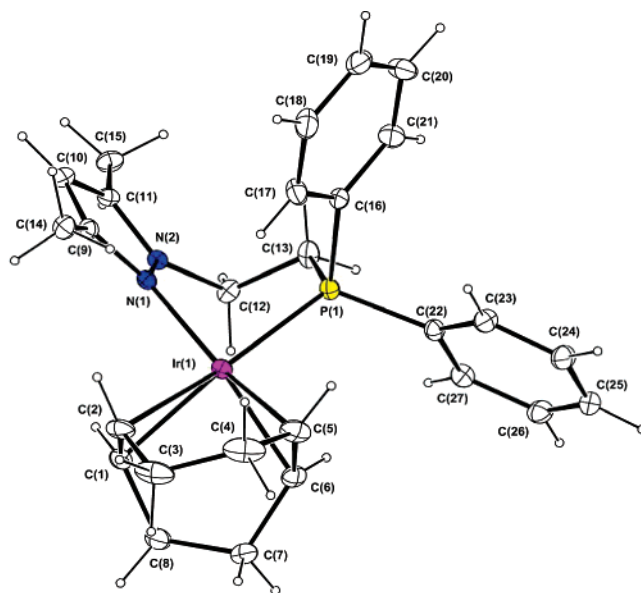


Figure 1. ORTEP depiction of the cationic fragment of [Ir(Me₂PyP)(COD)]BPh₄ (**3b**) at 20% thermal ellipsoids for the non-hydrogen atoms. Selected bond lengths (Å) and angles (deg): Ir(1)–P(1) = 2.2882(6); Ir(1)–N(1) = 2.1045(16); Ir(1)–C(1) = 2.2072(2); Ir(1)–C(2) = 2.33(2); Ir(1)–C(5) = 2.132(7); Ir(1)–C(6) = 2.140(2); C(1)–C(2) = 1.379(3); C(5)–C(6) = 1.408(3); P(1)–Ir(1)–N(1) = 84.31(5); P(1)–Ir(1)–C(5) = 93.73(7); P(1)–Ir(1)–C(6) = 95.99(6); N(1)–Ir(1)–C(1) = 91.43(7); N(1)–Ir(1)–C(2) = 96.69(8); C(1)–Ir(1)–C(6) = 81.05(8); C(2)–Ir(1)–C(5) = 80.62(10); C(1)–Ir(1)–C(5) = 96.92(9); C(2)–Ir(1)–C(6) = 87.92(9).

We have previously reported the solid-state structures of [M(PyP)(COD)]BPh₄ (M = Ir, **3a**; Rh, **4a**).⁵⁵ Single crystals of [Ir(Me₂PyP)(COD)]BPh₄ (**3b**), suitable for X-ray crystallography, were obtained by vapor diffusion of *n*-hexane to a THF solution of the complex. The solid-state structure of **3b** as determined by X-ray crystallography is shown in Figure 1 and is similar to the structure of **3a** and **4a**.⁵⁵

The coordination around the iridium center of **3b** is square planar. In the solid-state structures of **3a** and **4a** the bite angles of 89.47(6)° and 88.86(4)° respectively for P(1)–M(1)–N(1) (M = Ir, Rh)⁵⁵ are close to the ideal angle of 90° expected for square planar complexes, which implies a very low level of ring strain upon chelation of the PyP (**2a**) ligand. The rather acute bite angle of 84.31(5)° for [Ir(Me₂PyP)(COD)]BPh₄ (**3b**) is very similar to the value of 82.68(5)° reported by Esquiús et al.¹⁷ for the analogous rhodium complex [Rh(Me₂PyP)(COD)]BF₄. The deviation from the ideal value of 90° is probably due to steric effects imposed by the CH₃ group interacting with the COD ligand in **3b** and [Rh(Me₂PyP)(COD)]BF₄.

All of the six-membered metallacycles defined by M(1), Na(1), N(2), C(12), C(13), and P(1) in **3a**, **4a**,⁵⁵ and **3b** adopt pseudoboat conformations. Similar pseudoboat conformations have also been observed in the reported X-ray structures of related complexes.^{17,62} All of the M–N, M–P, and M–C bond distances (M = Ir, Rh, Table 2) are within the range reported in the literature for similar complexes.^{17,59,61–63}

Synthesis of Cationic Iridium Complexes with R₂PyP Ligands and Carbonyls as Co-ligands, [Ir(R₂PyP)(CO)₂]BPh₄. The cationic iridium(I) complexes [Ir(R₂PyP)(CO)₂]BPh₄

(62) Anderson, M. P.; Casalnuovo, A. L.; Johnson, B. J.; Mattson, B. M.; Mueiting, A. M.; Pignolet, L. H. *Inorg. Chem.* **1988**, *27*, 1649–1658.

(63) Yang, H.; Lugan, N.; Mathieu, R. *Organometallics* **1997**, *16*, 2089–2095.

Table 1. Infrared Carbonyl Stretching Frequencies,^a ¹³C{¹H} NMR (¹³CO Resonances), and ³¹P{¹H} NMR^b Chemical Shift Data for Neutral [M(R₂PyP)(CO)Cl] (M = Rh, Ir) Complexes

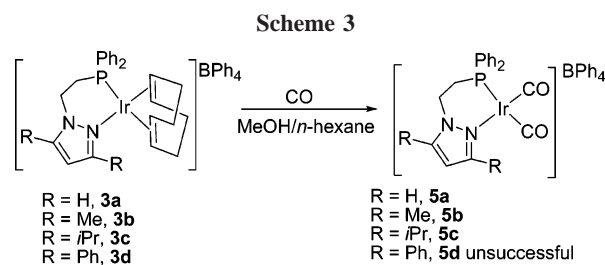
| iridium complex | $\nu(\text{CO})$ (cm ⁻¹) | ¹³ C (CO) ppm (² J _{P-C} Hz) | ³¹ P ppm |
|---|--------------------------------------|---|--|
| [Ir(PyP)(CO)Cl] (6a) ^c | 1983 | 174.4 (d, 13.8) | 10.4 |
| [Ir(Me ₂ PyP)(CO)Cl] (6b) | 1968 | 1175.8 (d, 12.6) | 13.5 |
| [Ir(<i>i</i> Pr ₂ PyP)(CO)Cl] (6c) | 1974 | 175.3 (d, 12.3) ^d | 13.8 |
| [Ir(Ph ₂ PyP)(CO)Cl] (6d) | 1949 | n/a | 14.8 |
| rhodium complex | $\nu(\text{CO})$ (cm ⁻¹) | ¹³ C (CO) ppm (¹ J _{Rh-C} , ² J _{P-C} Hz) | ³¹ P ppm (¹ J _{Rh-P} Hz) |
| [Rh(PyP)(CO)Cl] (7a) ^c | 1995 | 188.7 (dd, 71.2, 18.2) | 38.7 (165.5) |
| [Rh(Me ₂ PyP)(CO)Cl] (7b) | 1980 | 189.7 (dd, 72.7, 16.1) | 41.9 (163.8) |
| [Rh(<i>i</i> Pr ₂ PyP)(CO)Cl] (7c) | 1986 | 189.7 (dd, 72.1, 17.0) | 42.0 (163.8) |
| [Rh(Ph ₂ PyP)(CO)Cl] (7d) | 1980 | 188.4 (dd, 73.3, 6.9) ^e | 42.1 (164.5) ^e |

^a IR spectra were acquired using KBr disks. ^bSpectra were acquired in CD₂Cl₂. ^cComplexes **6a** and **7a** have been reported previously⁵⁵ and were included here for completeness. ^dSpectra were acquired at 240 K. ^eSpectra were acquired in CDCl₃.

Table 2. Selected Bond Lengths and Angles^a of the Inner Coordination Spheres of [Ir(PyP)(CO)Cl] (6a**), [Ir(Me₂PyP)(CO)Cl] (**6b**), [Ir(*i*Pr₂PyP)(CO)Cl] (**6c**), [Rh(PyP)(CO)Cl] (**7a**), [Rh(Me₂PyP)(CO)Cl] (**7b**), and [Rh(*i*Pr₂PyP)(CO)Cl]BPh₄ (**7c**)**

| atoms (M = Rh, Ir) | 6a ^b | 6b | 6c | 7a ^b | 7b | 7c |
|--------------------|------------------------|------------|-------------|------------------------|-------------|-------------|
| M(1)–P(1) | 2.2161(7) | 2.2120(17) | 2.2206(7) | 2.2150(7) | 2.2206(5) | 2.2256(7) |
| M(1)–N(1) | 2.119(2) | 2.110(4) | 2.1018(19) | 2.1233(18) | 2.1138(14) | 2.1185(16) |
| M(1)–C(1) | 1.811(3) | 1.806(6) | 1.808(2) | 1.798(3) | 1.8079(18) | 1.816(2) |
| M(1)–Cl(1) | 2.3890(7) | 2.4005(17) | 2.3947(7) | 2.3931(7) | 2.4030(5) | 2.4154(7) |
| C(1)–O(1) | 1.146(3) | 1.163(7) | 1.159(3) | 1.146(3) | 1.143(2) | 1.146(2) |
| P(1)–M(1)–N(1) | 93.21(5) | 86.77(13) | 87.56(5) | 92.93(5) | 81.83(4) | 87.52(5) |
| N(1)–M(1)–Cl(1) | 88.28(5) | 88.99(13) | 90.90(6) | 89.76(5) | 91.25(4) | 93.12(5) |
| Cl(1)–M(1)–C(1) | 89.72(8) | 92.48(19) | 91.29(7) | 88.86(8) | 93.98(6) | 89.68(6) |
| C(1)–M(1)–P(1) | 88.88(8) | 91.92(19) | 90.56(7) | 88.58(8) | 93.55(6) | 90.14(6) |
| N(1)–M(1)–C(1) | 175.40(10) | 178.1(2) | 176.20(8) | 174.93(10) | 175.35(7) | 175.06(7) |
| Cl(1)–M(1)–P(1) | 178.14(2) | 172.07(6) | 174.234(17) | 176.96(2) | 172.927(16) | 173.825(16) |

^a Estimated standard deviations in the least significant figures are given in parentheses. ^bThe solid-state structures of **7a** and **6a** were reported previously⁵⁵ and were included here for comparison.



(R = H, **5a**; Me, **5b**; *i*Pr, **5c**) were synthesized by the displacement of COD from [Ir(R₂PyP)(COD)]BPh₄ (R = H, Me, *i*Pr; **3a–3c**) in methanol/*n*-hexane suspensions under an atmosphere of carbon monoxide (Scheme 3) in the same manner as used in the synthesis of [Ir(PyP)(CO)₂]BPh₄ (**5a**).⁵⁵ Analogous reactions with the iridium complex [Ir(Ph₂PyP)(COD)]BPh₄ (**3d**) and rhodium complexes [Rh(R₂PyP)(COD)]BPh₄ (R = H, **4a**; R = Me, **4b**) were not successful.

Complexes **5a–5c** were isolated as mildly air-sensitive bright yellow solids. The IR spectra of **5a–5c** show two strong absorption bands of near equivalent intensity for the metal-bound carbonyls, consistent with the presence of two CO groups bound in a *cis* fashion to the metal center. Complexes **5a–5c**, while only mildly air sensitive, are unstable in solution at room temperature, particularly, in coordinating solvents such as THF or acetone. At room temperature, the ¹³C{¹H} NMR (125 MHz, CD₂Cl₂) spectrum of the ¹³CO-labeled complex [Ir(PyP)(¹³CO)₂]BPh₄ (**5a'**) contains two very broad resonances at 177.2 and 171.3 ppm due to the two ¹³CO groups, while resonances due to other ¹³C nuclei in the complex are sharp, and the ³¹P{¹H} NMR (202 MHz, CD₂Cl₂) spectrum shows a broad resonance that is devoid of any coupling to the two labeled carbonyls. At 215 K, relatively well-resolved resonances at 177.6 (d, ²J_{P-C} = 104.2 Hz, ¹³CO (*trans* to P)) and 170.6 (d, ²J_{P-C} = 11.2 Hz, ¹³CO (*cis* to P)) ppm were observed in the ¹³C{¹H} spectrum,

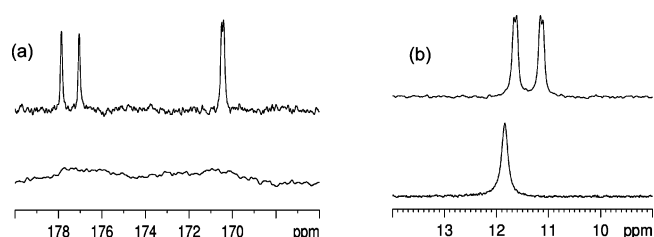
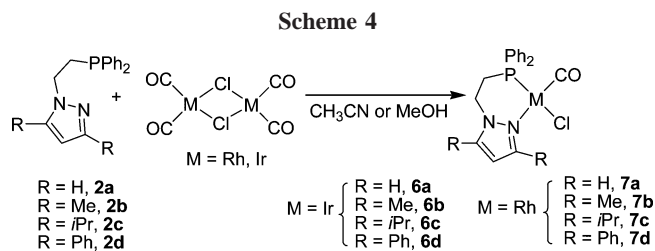


Figure 2. NMR spectra of [Ir(PyP)(¹³CO)₂]BPh₄ (**5a'**) in CD₂Cl₂. (a) Carbonyl region of the ¹³C{¹H} (125 MHz) spectra at 298 K (bottom) and 215 K (top); (b) ³¹P{¹H} (202 MHz) spectra at 298 K (bottom) and 215 K (top).

and a sharp resonance was observed in the ³¹P{¹H} spectrum at 11.4 ppm (dd, ²J_{13CO-P} = 104.2 Hz and ²J_{13CO-P} = 11.2 Hz) (Figure 2). These observations indicate that at room temperature the two carbonyl groups exchange with each other, possibly via a solvent-stabilized five-coordinate transition state, and the exchange is significantly slowed at 215 K. A similar exchange process was observed for an analogous rhodium complex, [Rh(PC)(¹³CO)₂]BPh₄, where PC = 3-[2-(diphenylphosphino)ethyl]-1-methylimidazol-2-ylidene.⁴⁸

Synthesis of Neutral Rhodium and Iridium Complexes with R₂PyP Ligands and Carbonyl and Chloride as Co-ligands [M(R₂PyP)(CO)Cl]. Neutral complexes of iridium (**6a–6d**) and rhodium (**7a–7d**) were synthesized by slow addition of a solution of the appropriate ligand to a solution of [M(μ -Cl)(CO)₂] (M = Rh or Ir, Scheme 4). All of the complexes were isolated as reasonably air-stable, pale yellow solids.

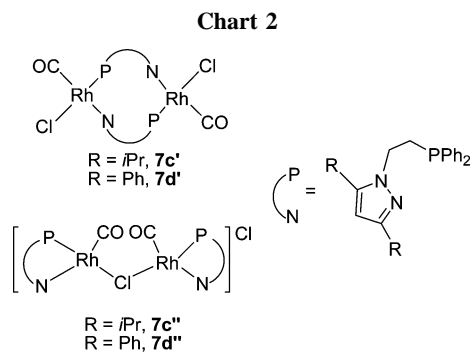
The stereochemistry around all the metal centers of these complexes has CO *cis* to P, i.e., *trans* to the N donor. The assignment of this stereochemistry is based on the $\nu(\text{CO})$ stretching frequencies in the IR spectra and the small ²J_{P-C} values (<20 Hz) observed for all complexes (Table 1). The



$\nu(\text{CO})$ values are in agreement with values reported in the literature for analogous complexes whose stereochemistry had been confirmed by X-ray crystallography.^{15,62} The CO ¹³C chemical shifts of these complexes, ²*J*_{P-CO} and ¹*J*_{Rh-CO} (Table 2), are all in agreement with previously reported similar complexes with the same stereochemistry.^{15,62} The observed stereochemistry can be rationalized as being due to the placement of the strongly π -accepting carbonyl ligand *trans* to the σ donor N. The mixing of the orbitals involved in the binding of these mutually *trans* ligands will best stabilize both the M–CO and the M–N bonds.⁶⁴

All of the metal complexes **6a–7d** were characterized by NMR spectroscopy. The NMR spectra of **6b–6d** and **7b–7d** indicate that the molecules are fluxional at room temperature due to ring flip of the six-membered metallacycle formed upon chelation of the bidentate P–N ligand. Low-temperature NMR was in these cases essential to undertake the full spectroscopic characterization of the complexes (Figure 3).

Formation of Highly Symmetrical Dinuclear Neutral Complexes. In the synthesis of neutral complexes **6a–7d**, it was essential that the ligand solution be added slowly for the clean formation of the monomeric complex. If the rate of ligand addition was not properly controlled, a mixture of two species, the monomer as well as a possibly dimeric compound, was formed (Chart 2, **7c'**, **7d'**, **7c''**, **7d''**). The formation of the second species occurred more readily in the case of the rhodium complexes than the iridium complexes and also occurred more readily in the cases where the substituents on the pyrazole ring were larger (*R*₂PyP, *R* = *i*Pr, Ph). Changing the reaction solvent from methanol to acetonitrile favored the formation of the



desired monomeric species. This was manifested most clearly in the successful synthesis, in acetonitrile solvent, of the monomeric complex $[\text{Rh}(i\text{Pr}_2\text{PyP})(\text{CO})\text{Cl}]$ (**7c**), whose solid-state structure was determined (see Figure 5).

The NMR, IR, and ESI-MS spectra and elemental analysis do not confidently allow the unambiguous assignment of the second species formed to either the neutral complexes **7c'** and **7d'** or the cationic complexes **7c''** and **7d''** (Chart 2). Because of the very similar spectroscopic data obtained for the dimer in comparison with the monomer, the most likely dimer formed was **7c'** and **7d'**. The low solubility of the dimer complexes in methanol suggests that they are unlikely to be of the form of the cationic complexes **7c''** and **7d''**.

Solid-State Structures of $[\text{M}(\text{Me}_2\text{PyP})(\text{CO})\text{Cl}]$ (*M* = Ir, **6b; Rh, **7b**) and $[\text{M}(i\text{Pr}_2\text{PyP})(\text{CO})\text{Cl}]$ (*M* = Ir, **6c**; Rh, **7c**).** Crystals of $[\text{M}(\text{Me}_2\text{PyP})(\text{CO})\text{Cl}]$ (*M* = Rh, **6b**; Ir, **7b**) and $[\text{M}(i\text{Pr}_2\text{PyP})(\text{CO})\text{Cl}]$ (*M* = Rh, **6c**; Ir, **7c**) suitable for X-ray analysis were obtained by layering a concentrated dichloromethane (*dcm*) or *dcm-d*₂ solution of the complexes with diethyl ether, *n*-pentane, or *n*-hexane. The ORTEP diagrams containing the atom-numbering schemes are shown in Figures 4 (**6b** and **7b**) and 5 (**6c** and **7c**), with selected bond lengths and bond angles presented in Table 2.

The solid-state structures unequivocally confirm the monomeric nature of these metal complexes, and similar monomeric structures could be assigned to the equivalent complexes reported here on the basis of the similarity in spectroscopic data. The solid-state structures of **6a**,⁵⁵ **6b**, **6c** and **7a**,⁵⁵ **7b**, **7c** are all similar, with the coordination spheres around the metal centers being slightly distorted square planar. The phosphorus and the CO ligands are positioned *cis* on the metal center, as was also observed for the solution structure using NMR.

All of the six-membered metallacycles defined by P(1)–C(6)–C(5)–N(2)–N(1)–M(1) adopt a similar highly distorted boat conformation in comparison to the conformation adopted in the equivalent cationic metal complexes with a COD coligand, **3a**, **4a**,⁵⁵ and **3b**. The P(1)–M(1)–N(1) (*M* = Rh and Ir) angles varied from 81.8° to 93.2° (Table 2) and decreased with the placement of substituents on the pyrazolyl ring of the ligand. These bite angles are similar to values reported in the literature for similar metal complexes.^{15,62} All of the remaining *cis* angles are close to the ideal orthogonal angles and fall within the range 88.3–94.0°. These *cis* angles increase with the increasing steric bulk of the pyrazolyl-C3/C5 substituents. The *trans* P–M–Cl and N–M–C angles ranging from 172° to 178° (Table 2) deviate more from the ideal value of 180° for square planar geometry as the size of the pyrazolyl-C3/C5 substituents increases. All the M–P, M–N, M–Cl, and M–C bond lengths (*M* = Ir, Rh) are within the reported values for similar

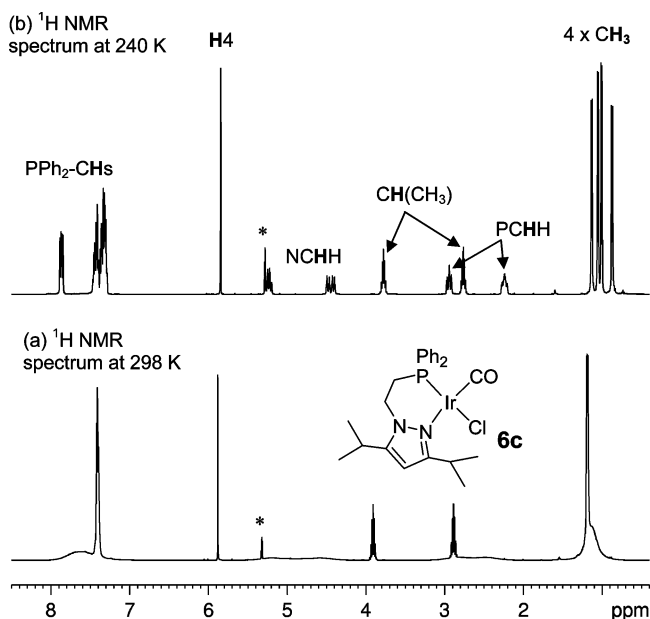


Figure 3. ¹H NMR spectra (500 MHz, CD₂Cl₂) of $[\text{Ir}(i\text{Pr}_2\text{PyP})(\text{CO})\text{Cl}]$ (**6c**) at (a) 298 K and (b) 240 K (* denotes the residual solvent resonance).

(64) Roundhill, D. M.; Bechtold, R. A.; Roundhill, S. G. N. *Inorg. Chem.* **1980**, *19*, 284–289.

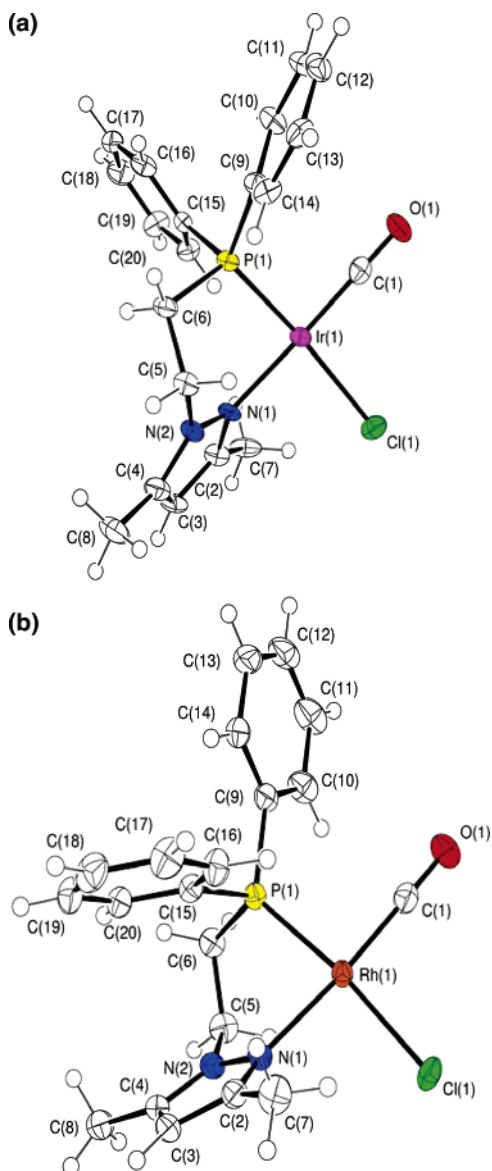


Figure 4. ORTEP depictions with atom-numbering schemes of (a) $[\text{Ir}(\text{Me}_2\text{PyP})(\text{CO})\text{Cl}]$ (**6b**) and (b) $[\text{Rh}(\text{Me}_2\text{PyP})(\text{CO})\text{Cl}]$ (**7b**) at 50% thermal ellipsoids for the non-hydrogen atoms.

complexes.^{15,62} The M–P bond lengths were observed to be shorter than those found in the equivalent cationic complexes with the COD co-ligand.

The M–N bond lengths in the solid-state structures of the neutral complexes $[\text{M}(\text{R}_2\text{PyP})(\text{CO})\text{Cl}]$ (M = Ir, R = Me, **6b** and R = *i*Pr, **6c**; M = Rh, R = Me, **7b** and R = *i*Pr, **7c**) were slightly shorter than the M–N bond lengths in the solid-state structure of the complexes containing the unsubstituted phosphine–pyrazolyl ligand, $[\text{M}(\text{PyP})(\text{CO})\text{Cl}]$ (M = Ir, **6a** and M = Rh, **7a**) (see Table 2). This was attributed to the stronger donor ability of the methyl- and isopropyl-substituted pyrazolyl donors resulting from the electron-donating properties of the methyl and isopropyl groups.

Catalytic Intramolecular Hydroamination. A range of the iridium and rhodium cationic, $[\text{M}(\text{R}_2\text{PyP})(\text{COD})]\text{BPh}_4$ and $[\text{M}(\text{R}_2\text{PyP})(\text{CO}_2)]\text{BPh}_4$, and neutral, $[\text{M}(\text{R}_2\text{PyP})(\text{CO})\text{Cl}]$, complexes described above were examined as catalysts for intramolecular hydroamination, by studying the cyclization of 4-pentyn-1-amine (**8**) to 2-methyl-1-pyrroline (**9**) (Scheme 5). 4-Pentyn-1-amine has been widely used as a substrate for studying

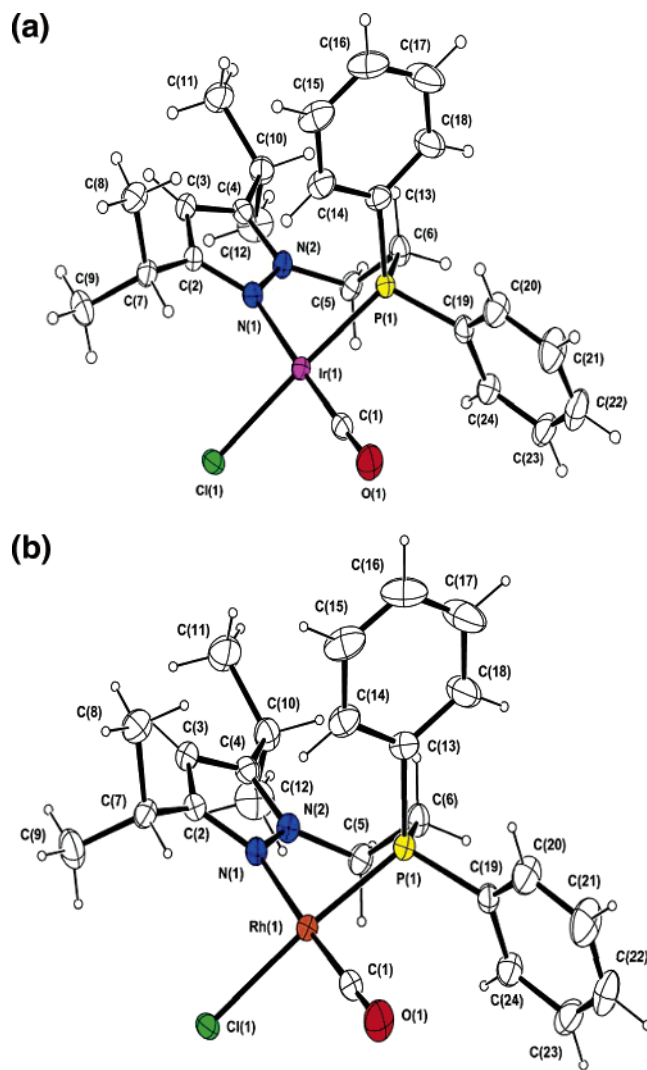
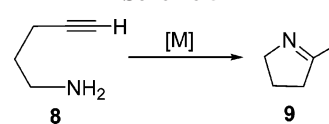


Figure 5. ORTEP depictions with atom-numbering schemes of (a) $[\text{Ir}(\text{iPr}_2\text{PyP})(\text{CO})\text{Cl}]$ (**6c**) and (b) $[\text{Rh}(\text{iPr}_2\text{PyP})(\text{CO})\text{Cl}]$ (**7c**) at 50% thermal ellipsoids for the non-hydrogen atoms.

Scheme 5



the intramolecular catalyzed hydroamination reaction^{37,42,49,65,66} and provides a good basis for comparison of catalyst efficiency.

Catalyzed Cyclization Using Iridium Cationic Complexes with Bidentate Phosphine–Pyrazolyl Ligands and COD as Co-ligands, $[\text{Ir}(\text{R}_2\text{PyP})(\text{COD})]\text{BPh}_4$ (3a–3d**).** The cationic iridium complexes $[\text{Ir}(\text{R}_2\text{PyP})(\text{COD})]\text{BPh}_4$ (**3a–3d**) were extremely efficient catalysts for the cyclization of 4-pentyn-1-amine (**8**) to 2-methyl-1-pyrroline (**9**). Using a catalyst loading of 1.2–1.5 mol % in CDCl_3 at 60 °C, the cyclization of **8** to **9** was complete within minutes. The calculated turnover rates at 50% conversions (N_t) range from 1200 to 3100 h^{-1} (Table 3). A similar N_t value was also observed when the cyclization using $[\text{Ir}(\text{PyP})(\text{COD})]\text{BPh}_4$ (**3a**) was conducted in THF-d_8 . These turnover rates are significantly higher than any of the rates reported to date for late transition metal complexes in promoting the cyclization of 4-pentyn-1-amine (**8**).^{37,42,66–68}

(65) Panda, T. K.; Zulys, A.; Gainer, M. T.; Roesky, P. W. *Organometallics* **2005**, *24*, 2197–2202.

(66) Li, Y.-W.; Marks, T. J. *J. Am. Chem. Soc.* **1996**, *118*, 9295–9306.

Table 3. Catalytic Efficiency of Cationic Iridium Complexes [Ir(R₂PyP)(COD)]BPh₄ (R = H, **3a; Me, **3b**; *i*Pr, **3c**; and Ph, **3d**) for the Cyclization of 4-Pentyn-1-amine (**8**) to 2-Methyl-1-pyrroline (**9**)^a**

| complex | mol % | <i>N_t</i> (h ⁻¹) ^b | time (h) at >98% conv |
|--|-------|--|-----------------------|
| [Ir(PyP)(COD)]BPh ₄ (3a) ^c | 1.4 | 1800 | 0.50 |
| [Ir(PyP)(COD)]BPh ₄ (3a) | 1.4 | 1200 | 1.50 |
| [Ir(PyP)(COD)]BPh ₄ (3b) | 1.2 | 2250 | 0.25 |
| [Ir(Me ₂ PyP)(COD)]BPh ₄ (3c) | 1.4 | 3100 | 0.17 |
| [Ir(Ph ₂ PyP)(COD)]BPh ₄ (3d) | 1.5 | 1800 | 0.20 |
| [Ir(PyP)(COD)]BPh ₄ (3a) ^d | 1.5 | 400 | 1.00 |

^a Reactions were performed in CDCl₃ at 60 °C. ^b*N_t* (at 50% conversion) are estimated from time course profiles (see Supporting Information). ^c Reactions were performed in THF-*d*₈ at 60 °C. ^d Reaction was performed in CDCl₃ at room temperature.

The *N_t* values for cyclization promoted by [Ir(R₂PyP)(COD)]BPh₄ (**3a–3d**) vary with the substituents on the pyrazolyl donor following the trend *i*Pr > Me > Ph > H; that is, an increase in the steric bulk of R correlates with an increase in catalytic activity of the resulting metal complexes. This observation suggests that the catalyst efficiency is specifically dependent on crowding at the metal center.

At an early stage of the cyclization of 4-pentyn-1-amine (**8**) to 2-methyl-1-pyrroline (**9**) catalyzed by [Ir(R₂PyP)(COD)]BPh₄ (R = H, **3a**; Me, **3b**), the dissociation of the COD co-ligand was observed. Resonances due to free COD were observed in the ¹H NMR spectra, and ESI-MS performed on the reaction mixtures on completion of the catalytic reactions showed the presence of ions corresponding to the iridium catalyst with product molecules bound to [Ir(R₂PyP)(2-methyl-1-pyrroline)_{*n*}]⁺ (*n* = 1–3, R = H and Me), further confirming the dissociation of the COD co-ligand. This suggests that the loss of COD may be necessary to form the catalytically active species and also that the product could become involved in the catalytic cycle.

Catalyst Lifetime. The lifetime of the highly active catalyst [Ir(PyP)(COD)]BPh₄ (**3a**) in promoting the cyclization of 4-pentyn-1-amine to 2-methyl-1-pyrroline (at 1.4 mol %, in THF-*d*₈ at 60 °C) was investigated by the addition of a second aliquot of substrate after the complete conversion of the first aliquot of substrate to product, as observed by ¹H NMR spectroscopy, and the catalyst **3a** remained highly active in promoting the transformation of **8** to **9**. Where the turnover rate, *N_t*, for first aliquot of substrate was approximately 1800 h⁻¹, the *N_t* for the second aliquot was, however, about 6-fold less at 300 h⁻¹. The rate of cyclization for the second addition of substrate also slowed significantly after reaching about 80% conversion (180% total conversion), and complete conversion was reached only after approximately 600 min. The observed decrease in turnover rate with time is attributed to product inhibition, as has been established using closely related complexes as catalysts for the transformation of the same substrate.^{49,53} The product, 2-methylpyrroline, competitively inhibits the reaction, and as its concentration builds up in the reaction mixture, the catalyst efficiency decreases.

In a similar fashion, a second and third aliquot of substrate were added into the [Ir(Me₂PyP)(COD)]BPh₄ (**3b**)-promoted cyclization of **8** (Figure 6). The reaction profile and the turnover rates, *N_t*, clearly show that the rates decrease with subsequent additions of aliquots of substrate. The decrease in *N_t* from the

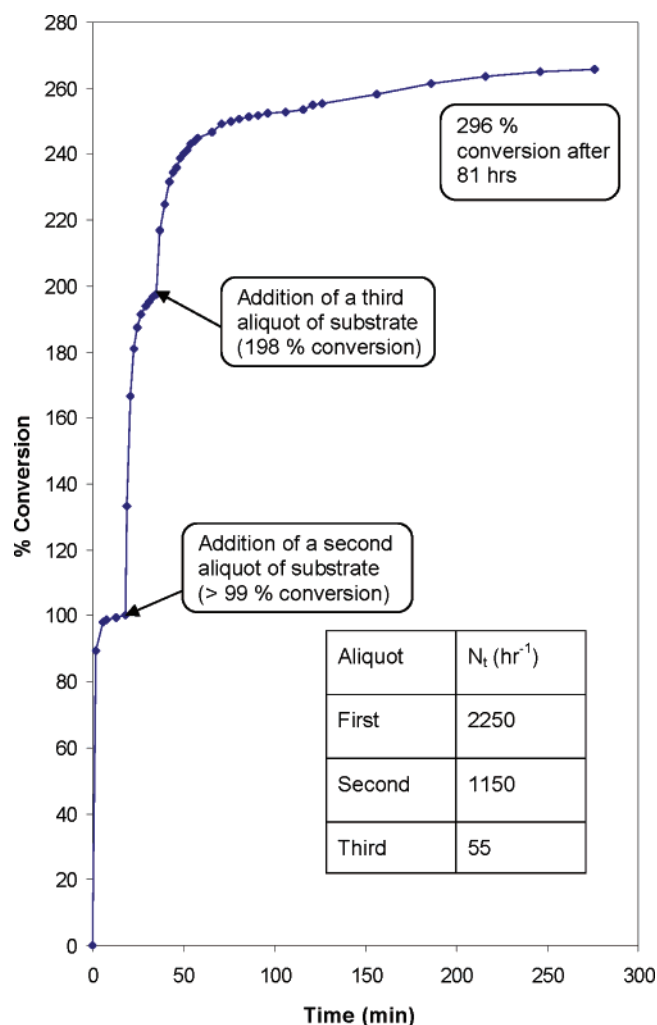


Figure 6. Reaction profile of the [Ir(Me₂PyP)(COD)]BPh₄ (**3b**) (1.2 mol % in CDCl₃ at 60 °C) catalyzed cyclization of 4-pentyn-1-amine to 2-methyl-1-pyrroline with the addition of a second (at 100% conversion) and third (at 198% conversion) aliquot of the amine.

first to the second addition of substrate was only approximately 2-fold. The turnover rate for the third substrate aliquot was found to be 20-fold lower than the rate observed for the second aliquot of substrate. The result here illustrates that the catalyst **3b** has a reasonably long lifetime at low catalyst loading (1.2 mol %), even though the catalytic efficiency decreases slowly through either deactivation of the catalyst or product inhibition of the cyclization reaction.

In short, air-stable metal complexes [Ir(R₂PyP)(COD)]BPh₄ (R = H, Me, *i*Pr, Ph; **3a–3d**) were demonstrated to be extremely efficient as catalysts for the intramolecular hydroamination of alkynes using 4-pentyn-1-amine (**8**) as the model substrate. These catalysts were also demonstrated to have long lifetimes with near quantitative conversion achieved for three consecutive additions of substrate. The catalyst [Ir(PyP)(COD)]BPh₄ (**3a**) is highly reactive even at room temperature.

Catalyzed Cyclization Using Cationic Rhodium Complex [Rh(PyP)(COD)]BPh₄ (4a**).** The efficiency of rhodium complex [Rh(PyP)(COD)]BPh₄ (**4a**) in promoting the intramolecular hydroamination of 4-pentyn-1-amine (**8**) was also investigated. In contrast with the high activity shown for the iridium analogue **3a**, the turnover rate observed using rhodium complex **4a** for the cyclization of **8** was only 3 h⁻¹. The reaction was incomplete even after 3 days at 60 °C.

(67) McGrane, P. L.; Livinghouse, T. *J. Am. Chem. Soc.* **1993**, *115*, 11485–11489.

(68) Bürgstein, M. R.; Berberich, H.; Roesky, P. W. *Chem.–Eur. J.* **2001**, *7*, 3078–3085.

Table 4. Catalytic Efficiency of [Ir(R₂PyP)(CO)₂]BPh₄ (R = H, **5a; Me, **5b**; and *i*Pr, **5c**) and [Ir(bpm)(CO)₂]BPh₄ for the Catalyzed Cyclization of 4-Pentyn-1-amine to 2-Methyl-1-pyrroline^a**

| catalyst | mol % | <i>N_t</i> (h ⁻¹) | time (h) at >98% conv |
|---|-------|---|-----------------------|
| [Ir(PyP)(CO) ₂]BPh ₄ (5a) | 1.3 | 11 | 38.0 |
| [Ir(Me ₂ PyP)(CO) ₂]BPh ₄ (5b) | 1.5 | 35 | 11.0 |
| [Ir(<i>i</i> Pr ₂ PyP)(CO) ₂]BPh ₄ (5c) | 1.5 | 26 | 10.5 |
| [Ir(bpm)(CO) ₂]BPh ₄ ^b | 1.5 | 50 | 2.2 |

^a Reactions were performed in CDCl₃ at 60 °C. ^bThe reaction was performed in THF-*d*₈ by Burling, S.⁴⁹

Catalyzed Cyclization Using Cationic Iridium Complexes with Bidentate Phosphine–Pyrazolyl Ligands and Carbonyls as Co-ligands. The efficiency of a series of iridium complexes [Ir(R₂PyP)(CO)₂]BPh₄ (R = H, **5a**; Me, **5b**; *i*Pr, **5c**) as catalysts for the catalyzed cyclization of 4-pentyn-1-amine (**8**) to 2-methyl-1-pyrroline (**9**) was also investigated (Table 4). Complete conversions of substrate to product were achieved in all cases. The complexes **5a–5c** are however much less efficient when compared with the catalytic activity of the analogous complexes having COD as co-ligands, [Ir(R₂PyP)(COD)]BPh₄ (**3a–3d**) (Table 4).

The presence of bulky R substituents on the pyrazolyl ring of the bidentate ligands R₂PyP (R = **2a**; R = Me, **2b**; R = *i*Pr, **2c**) significantly alters the catalytic reactivity of the resulting metal complexes [Ir(R₂PyP)(CO)₂]BPh₄ (**5a–5c**) for the cyclization of 4-pentyn-1-amine (**8**). As the substituent on the pyrazolyl ring of the phosphine–pyrazolyl ligands R₂PyP of [Ir(R₂PyP)(CO)₂]BPh₄ changes from R = H to R = Me, the turnover rate (*N_t*) increased by a factor of more than 3, and the time taken to reach complete conversion (*t_c*) decreased in a corresponding fashion. Further increases in the size of R to *i*Pr led to a drop in conversion rate. The conversion rates are all low and there is no clear correlation of catalyst activity to the nature of the substituents. The IR stretching frequencies of the metal-bound carbonyls of these complexes also do not show any clear correlation to the variation in catalytic efficiency.

The analogous complex containing the bidentate nitrogen donor ligand [Ir(bpm)(CO)₂]BPh₄ (where bpm = bis(1-pyrazolyl)methane), in THF-*d*₈ solvent, was reported by Field, Messerle, and co-workers⁴⁹ to be more efficient than the complexes **5a–5c** (in catalyzing the cyclization of 4-pentyn-1-amine (**8**)) (Table 4). The complex [Ir(bpm)(COD)]BPh₄ (in THF-*d*₈), with COD as co-ligand, was ineffective for the cyclization of 4-pentyn-1-amine (**8**) (1.5 mol %, 92% after 24.0 h).⁶⁹ This contrasts with the analogous complexes with bidentate phosphine–pyrazolyl ligands [Ir(R₂PyP)(COD)]BPh₄ (**3a–3d**), which were extremely efficient for this transformation (Table 3 above) and much more efficient than the analogous complexes with CO co-ligands. There is a clear difference between the bidentate COD and a pair of carbonyls in the catalytic activity of the complexes, and this identifies the importance of these co-ligands in the catalytic activity of the metal complexes.

Catalyzed Cyclization Using Neutral Iridium Complexes with Bidentate Phosphine–Pyrazolyl Ligands. The neutral complex [Ir(PyP)(CO)Cl] (**6a**) was a very inefficient catalyst for the cyclization of 4-pentyn-1-amine (**8**), and complete conversion of **8** to 2-methyl-1-pyrroline (**9**) was not achieved using either CDCl₃ (1.5 mol % catalyst, 60 °C, 50% conversion after 63 h) or THF-*d*₈ (1.7 mol % catalyst, 60 °C, 18%

conversion after 14.0 h) as the solvent. The neutral rhodium complex [Rh(PyP)(CO)Cl] (**7a**) was also found to be ineffective in catalyzing the cyclization of **8** (1.5 mol %, CDCl₃, 60 °C, 72% conversion after 45 h).

In comparing the efficiency of all three iridium complexes with the phosphine–pyrazolyl bidentate ligand PyP (**2a**) and different co-ligands [Ir(PyP)(COD)]BPh₄ (**3a**), [Ir(PyP)(CO)₂]BPh₄ (**5a**), and [Ir(PyP)(CO)Cl] (**6a**) as catalysts for the cyclization of 4-pentyn-1-amine (**8**), it was found that (i) the cationic complex [Ir(PyP)(COD)]BPh₄ (**3a**) with a COD co-ligand was extremely efficient in catalyzing the cyclization of **8**; (ii) the cationic complex [Ir(PyP)(CO)₂]BPh₄ (**5a**) with carbonyls as co-ligands is much less efficient when compared with **3a** but is still able to promote the complete conversion of **8** to 2-methyl-1-pyrroline (**9**) with reasonable efficiency; and (iii) the neutral complex [Ir(PyP)(CO)Cl] (**6a**) is not an effective catalyst for promoting this transformation.

Conclusions

This paper reports the synthesis of a series of bidentate phosphine–pyrazolyl donor ligands and some cationic and neutral complexes [M(R₂PyP)(COD)]BPh₄ (M = Ir and Rh, R = Me, *i*Pr, and Ph, **3a–4d**), [Ir(R₂PyP)(CO)₂]BPh₄ (R = Me, *i*Pr, and Ph; **5a–5c**), and [M(R₂PyP)(CO)Cl] (M = Ir and Rh, R = Me, *i*Pr, and Ph **6a–7d**). The solid-state structures of complexes [Ir(Me₂PyP)(COD)]BPh₄ (**3b**), [M(Me₂PyP)(CO)Cl] (M = Ir, **6b**; Rh, **7b**), and [M(*i*Pr₂PyP)(CO)Cl] (M = Ir, **6c**; Rh, **7c**) were determined by single-crystal diffraction analysis. In all of these structures the coordination around the metal center is square planar, as expected for four-coordinate Rh(I) and Ir(I) complexes. In all cases, the metallacycles formed upon chelation of bidentate phosphine–pyrazolyl donor ligands adopt distorted boat conformations.

The cationic iridium complexes with phosphine–pyrazolyl donor ligands and a COD co-ligand [Ir(R₂PyP)(COD)]BPh₄ (**3a–3d**) are very efficient in promoting the cyclization of **8** to **9** under mild conditions and are among the most efficient catalysts reported in the literature to date for the same transformation. These complexes also have long catalytic lifetimes and are effective even at ambient temperature. The high efficiency of [Ir(R₂PyP)(COD)]BPh₄ (**3a–3d**) is undoubtedly the result of a balance of both electronic and steric factors brought about from the choice of the metal, ligand, co-ligand, counterion, and substrate. The scope of applications of these complexes as general catalysts for hydroamination and mechanistic studies of the hydroamination reaction using these catalysts are underway in our laboratory.

The effect of the systematic modification of the pyrazolyl donor of the phosphine–pyrazolyl donor ligands on the catalytic efficiency for the hydroamination of 4-pentyn-1-amine of the resulting metal complexes has been demonstrated. Placing sterically demanding substituents (R) on the pyrazolyl ring of bidentate phosphine–pyrazolyl ligands in complexes [Ir(R₂PyP)(COD)]BPh₄ (**3a–3d**) varied the relative catalyst efficiency following the trend *i*Pr > Me > Ph > H. An increase in the steric bulk of R correlates directly with an increase in catalytic activity of the resulting metal complexes. The cationic iridium complexes with COD as the co-ligand, [Ir(R₂PyP)(COD)]BPh₄, were much more efficient than the corresponding complexes with CO co-ligands.

The neutral complexes [Ir(PyP)(CO)Cl] (**6a**) and [Rh(PyP)(CO)Cl] (**7a**) are catalytically active, but are poor catalysts for the conversion of **8** to **9** when compared with the cationic analogues [Ir(PyP)(CO)₂]BPh₄ (**5a**) and [Ir(PyP)(COD)]BPh₄

(69) Burling, S.; Field, L. D.; Messerle, B. A.; Wren, S. L. In *IC03-Conference of the Inorganic Division of the Royal Australian Chemical Institute*; The University of Melbourne: Australia, 2003; p P154.

(3a). The rhodium complexes with COD as co-ligands [Rh-(PyP)(COD)]BPh₄ (4a) do not have the high efficiency observed for the [Ir(R₂PyP)(COD)]BPh₄ (3a–3d) series in promoting the hydroamination of 4-pentyn-1-amine.

Experimental Section

General Considerations. All manipulations of metal complexes and air-sensitive reagents were carried out using standard Schlenk techniques or in a nitrogen-filled drybox. All solvents were distilled under an atmosphere of nitrogen. Diethyl ether, THF, THF-*d*₈, *n*-hexane, *n*-pentane, and benzene were distilled from sodium benzophenone ketyl. Dichloromethane was distilled from calcium hydride. Methanol was distilled from dimethoxymagnesium. CDCl₃ and CD₂Cl₂ were dried over calcium hydride and vacuum distilled before use. All compressed gases were obtained from British Oxygen Company (BOC gases) and Linde Gas Pty. Ltd. Nitrogen (>99.5%) and carbon monoxide (>99.5%) were used as supplied without purification. Pyrazole, 3,5-dimethylpyrazole, 1,2-dibromoethane (1,2-DBE), tetrabutylammonium bromide (TBAB), 1,5-cyclooctadiene (COD), *cis*-cyclooctene (COE), and sodium tetraphenylborate were obtained from Aldrich or Lancaster and used without further purification. Iridium(III) chloride hydrate and rhodium(III) chloride hydrate were obtained from Precious Metals Online, PMO P/L, and were used without further purification. [Ir(μ -Cl)(COD)]₂,⁷⁰ [Rh(μ -Cl)(COD)]₂,⁷¹ [Rh(μ -Cl)(CO)]₂,⁷² [Ir(μ -Cl)(COE)]₂,⁷⁰ [Ir(bpm)(CO)]₂BPh₄,⁷³ 3,5-diphenylpyrazole,^{74,75} diphenylphosphine,⁷⁶ and 4-pentyn-1-amine⁷⁷ were prepared by literature methods.

¹H, ³¹P, and ¹³C NMR spectra were recorded on Bruker DPX300 or DMX500 spectrometers, operating at 300 or 500 MHz, 121 MHz (³¹P), and 75 or 125 MHz (¹³C). All spectra were recorded at 298 K unless otherwise specified. ¹H NMR and ¹³C NMR chemical shifts were referenced internally to residual solvent resonances. ³¹P NMR was referenced externally using H₃PO₄ (85% in D₂O) in a capillary. Electrospray mass spectra were recorded on a Finnigan LQC or a Finnigan Micromass QToF mass spectrometer.

Melting points were recorded using a Mel-Temp apparatus and are uncorrected. IR spectra were recorded using an ATI Mattson Genesis Series FTIR spectrometer or an Avatar370 FTIR spectrometer. Elemental analyses were performed by the Campbell Microanalytical Laboratory at the University of Otago, New Zealand. Single-crystal X-ray structure analyses were done at the X-ray Crystallography Centre, the University of Sydney, Australia.

General Procedure for Catalytic Hydroamination. Metal complex catalyzed intramolecular hydroamination reactions were performed on a small scale in NMR tubes fitted with a Youngs concentric Teflon valve. 4-Pentyn-1-amine was added to a solution of the catalyst in deuterated solvent (CDCl₃ or THF-*d*₈, 0.6–0.7 mL) in an NMR tube at RT, and the sample was kept frozen in liquid nitrogen until the acquisition of ¹H NMR spectra was started. The solvent was freshly vacuum-transferred into an NMR tube containing the catalyst prior to the addition of the substrate. Most of the reactions were performed with approximately 1.5 mol % of catalyst loading, at 60 °C by heating the sample in an oil bath maintained at 60 °C or by heating at 60 °C within the probe of the

NMR spectrometer. Room-temperature means 298 K (25 °C) in catalytic reactions. ¹H NMR spectra were recorded with a relaxation delay of 5 s, and the conversion of substrate to product was determined by integration of the product resonances relative to the substrate resonances in the ¹H NMR spectra. Complete conversion (>98%) was taken to be the time where no remaining substrate resonances were evident. The turnover rate (*N_t* h⁻¹) was calculated as the number of moles of product/mole of catalyst/hour and was calculated at the point of 50% conversion.

Synthesis of Ligands. Synthesis 1-(2-Bromoethyl)pyrazoles (1b–1d). Compounds 1b and 1d were synthesized using a method analogous to the preparation of 1-(2-bromoethyl)pyrazole (1a).⁵⁵ The synthesis of 1-(2-bromoethyl)-3,5-dimethylpyrazole (1b) is presented here, and the preparation of 1-(2-bromoethyl)-3,5-diisopropylpyrazole (1c) and 1-(2-bromoethyl)-3,5-diphenylpyrazole (1d) are provided in the Supporting Information.

1-(2-Bromoethyl)-3,5-dimethylpyrazole (1b). Aqueous sodium hydroxide (30 mL, 40% (w/v), 300 mmol) was added to a mixture of 3,5-dimethylpyrazole (9.61 g, 100 mmol), TBAB (3.22 g, 10.0 mmol), and 1,2-DBE (216 mL, 2.50 mol). After the reaction mixture was heated for 20 h at 60 °C with vigorous stirring, it was cooled to RT and water (60 mL) was added. The organic layer was separated, washed with water (60 mL), dried over anhydrous calcium chloride, and filtered, and the solvent was removed *in vacuo* to give a pale yellow liquid. The product was purified by either vacuum distillation through a Vigreux column or by column chromatography (ethyl acetate). Yield: 10.6 g (52%). Bp: 83–85 °C/2 mmHg; lit.⁵⁷ 46–48 °C/0.05 mmHg. ¹H NMR (300 MHz, CDCl₃): δ 5.79 (s, 1H, H₄), 4.31 (t, ³J_{CH₂Br-CH₂N} = 6.8 Hz, 2H, NCH₂), 3.68 (t, ³J_{NCH₂-CH₂Br} = 6.8 Hz, 2H, CH₂Br), 2.26 (s, 3H, C5CH₃), 2.21 (s, 3H, C3CH₃) ppm. ¹³C{¹H} NMR (75 MHz, CDCl₃): δ 148.5 (C3), 139.6 (C5), 105.3 (C4), 49.8 (NCH₂), 30.5 (CH₂Br), 13.6 (C3CH₃), 11.2 (C5CH₃) ppm. IR (neat, NaCl plates): ν 3032 (w), 2954 (m), 2921 (m), 2843 (w), 1555 (s), 1462 (s), 1424 (s), 1388 (m), 1302 (s), 1261 (m), 1032 (w), 779 (m) cm⁻¹.

Synthesis of 1-[2-(Diphenylphosphino)ethyl]pyrazoles, R₂PyP (R = Me, *i*Pr, and Ph; 2b–2d). Compounds 2b–2d were synthesized using a method analogous to that used for the synthesis of 1-[2-(diphenylphosphino)ethyl]pyrazole (2a).⁵⁵ A representative example is presented here, and the detailed syntheses of 2c and 2d are provided in the Supporting Information.

3,5-Dimethyl-1-[2-(Diphenylphosphino)ethyl]pyrazole, Me₂PyP (2b). *n*-Butyllithium (1.4 M in hexanes, 11.0 mL, 15.0 mmol) was added slowly to a solution of diphenylphosphine (2.61 mL, 15.0 mmol) in tetrahydrofuran (40 mL) at -70 °C, and the resulting red solution was stirred at this temperature for a further 30 min and then at 0 °C for 1 h. The diphenylphosphide solution was transferred slowly to a solution of 1-(2-bromoethyl)-3,5-dimethylpyrazole (1b, 3.05 g, 15.0 mmol) in THF (40 mL) at 0 °C, and the reaction mixture was stirred at RT under nitrogen overnight. THF was removed *in vacuo*, and benzene (70 mL) and deoxygenated water (30 mL) were added. The organic layer was separated, washed with deoxygenated water (2 × 20 mL), dried over anhydrous magnesium sulfate, and filtered, and the solvent was removed *in vacuo*. Unreacted diphenylphosphine was removed by vacuum distillation to afford 3,5-dimethyl-1-[2-(diphenylphosphino)ethyl]pyrazole (2b) as a viscous, colorless oil. Yield: 3.67 g (79%); lit.¹⁷ mp 20–22 °C. MS (EI), *m/z* (%): 308 (11) [M]⁺, 231 (100) [M - Ph]⁺, 212 (73), 183 (49), 108 (36). HRMS: found 308.1443, calcd for C₁₉H₂₁N₂P 308.1442. ¹H NMR (500 MHz, C₆D₆): δ 7.37–7.33 (m, 4H, *o*-CH of PPh₂), 7.05–7.00 (m, 6H, *m*- and *p*-CH of PPh₂), 5.67 (s, 1H, H₄), 3.94 (m, 2H, NCH₂), 2.50 (m, 2H, PCH₂), 2.32 (s, 3H, C3CH₃), 1.68 (s, 3H, C5CH₃) ppm. ³¹P{¹H} NMR (121 MHz, C₆D₆): δ -21.0 ppm. ¹³C{¹H} NMR (75 MHz, C₆D₆): δ 147.6 (s, C3), 138.9 (d, ¹J_{P-C} = 13.5 Hz, *ipso*-C of PPh₂), 138.2 (s, C5), 133.4 (d, ²J_{P-C} = 18.9 Hz, *o*-C of PPh₂), 129.2 (s,

(70) Herde, J. L.; Lambert, J. C.; Senoff, C. V. *Inorg. Synth.* **1974**, *14*, 18–20.

(71) Giordano, G. C.; Crabtree, R. H. *Inorg. Synth.* **1990**, *28*, 88–90.

(72) McCleverty, J. A.; Wilkinson, G. *Inorg. Synth.* **1990**, *28*, 84–86.

(73) Field, L. D.; Messerle, B. A.; Rehr, M.; Soler, L. P.; Hambley, T. W. *Organometallics* **2003**, *22*, 2387–2395.

(74) Kitajima, N.; Fujisawa, K.; Fujimoto, C.; Morooka, Y.; Hashimoto, S.; Kitagawa, T.; Toriumi, K.; Tatsumi, K.; Nakamura, A. *J. Am. Chem. Soc.* **1992**, *114*, 1277–1291.

(75) Walworth, B. L.; Klingsberg, E. (American Cyanamid Co.). U.S. Patent US3922161, 1975.

(76) Bianco, V. D.; Doronzo, S. *Inorg. Synth.* **1976**, *16*, 161–163.

(77) Field, L. D.; Morgan, J. Manuscript in preparation.

p-C of PPh₂), 129.1 (d, ³J_{P-C} = 8.8 Hz, *m*-C of PPh₂), 105.3 (s, C4), 46.0 (d, ²J_{P-C} = 25.0 Hz, NCH₂), 30.3 (d, ¹J_{P-C} = 14.9 Hz, PCH₂), 14.3 (s, C3CH₃), 10.9 (s, C5CH₃) ppm. IR (neat, NaCl plates): ν 3070 (m), 3052 (m), 2977 (m), 2919 (m), 1552 (s), 1481 (s), 1461 (s), 1422 (s), 1386 (m), 1307 (w), 1026 (w), 776 (w), 740 (s), 697 (s) cm⁻¹.

Synthesis of Metal Complexes. Synthesis of Cationic Iridium and Rhodium Complexes with Phosphine–Pyrazolyl Bidentate Ligands and 1,5-Cyclooctadiene as Co-ligands, [Ir(R₂PyP)(COD)]BPh₄ (R = H, Me, *i*Pr, and Ph). The synthesis of the cationic complex [Ir(PyP)(COD)]BPh₄ (**3a**) was performed using a modified literature method⁵⁵ and is presented here. The syntheses of [Ir(R₂PyP)(COD)]BPh₄ (R = Me, *i*Pr, and Ph, **3b–3d**) and [Rh(R₂PyP)(COD)]BPh₄ (R = H, Me, *i*Pr, and Ph, **4a–4d**) were carried out in a similar manner and are included in the Supporting Information.

[Ir(PyP)(COD)]BPh₄ (3a**).** A solution of **2a** (1.15 g, 4.10 mmol) in methanol (40 mL) was added slowly over 20 min to a suspension of [Ir(μ-Cl)(COD)]₂ (1.38 g, 2.06 mmol) in methanol (60 mL), and the orange-red solution obtained was stirred at RT for 45 min under an atmosphere of nitrogen. Sodium tetraphenylborate (1.41 g, 4.11 mmol) was added, an orange precipitate formed, and the reaction mixture was stirred for 3 h at RT. About 40% of the methanol was removed under reduced pressure, and the solid was collected by filtration, washed with methanol (5 × 7 mL) and *n*-pentane (5 × 9 mL), and dried under vacuum. Yield: 3.53 g (96%). Mp: 185–186 °C (dec). ESI-MS (MeOH), *m/z* (%): ES⁺, 581.2 (100) [M]⁺; ES⁻, 319.6 (100) BPh₄⁻. Anal. Found: C, 64.80; H, 5.40; N, 3.26. Calcd for C₄₉H₄₉BiRn₂P: C, 65.40; H, 5.49; N, 3.11. ¹H NMR (300 MHz, CD₂Cl₂): δ 7.56 (d, ³J_{H4-H3} = 2.3 Hz, 1H, H3), 7.54–7.40 (m, 10H, CH of PPh₂), 7.39–7.33 (br m, 8H, *o*-CH of BPh₄), 7.20 (d, ³J_{H4-H5} = 2.4 Hz, 1H, H5), 7.03 (t, ³J = 7.2 Hz, 8H, *m*-CH of BPh₄), 6.88 (t, ³J = 7.2 Hz, 4H, *p*-CH of BPh₄), 6.32 (apparent t, ³J_{H3-H4,H5-H4} = 2.3 Hz, 1H, H4), 4.95 (br, 2H, CH (*trans* to P) of COD), 4.29 (m, 2H, NCH₂), 3.19 (br, 2H, CH (*cis* to P) of COD), 2.44 (m, 2H, PCH₂), 2.39–2.22 (br, 4H, CHH (2H, *trans* to P) and CHH (2H, *cis* to P) of COD), 2.17–1.93 (br, 4H, CHH (2H, *trans* to P) and CHH (2H, *cis* to P) of COD) ppm. ³¹P{¹H} NMR (121 MHz, CD₂Cl₂): δ 10.5 ppm. ¹³C{¹H} NMR (75 MHz, CD₂Cl₂): δ 163.9 (q, ¹J_{B-C} = 49.4 Hz, *ipso*-C of BPh₄), 141.6 (s, C3), 135.8 (s, *o*-C of BPh₄), 134.7 (s, C5), 133.1 (d, *J*_{P-C} = 10.9 Hz, *o*-C or *m*-C of PPh₂), 131.4 (d, ⁴J_{P-C} = 2.2 Hz, *p*-C of PPh₂), 129.5 (d, ¹J_{P-C} = 54.3 Hz, *ipso*-C of PPh₂), 129.1 (d, *J*_{P-C} = 10.2 Hz, *m*-C or *o*-C of PPh₂), 125.6 (q, ⁴J_{B-C} = 2.9 Hz, *m*-C of BPh₄), 121.7 (s, *p*-C of BPh₄), 108.0 (s, C4), 95.3 (d, ²J_{P-C} = 11.6 Hz, CH (*trans* to P) of COD), 64.1 (s, CH (*cis* to P) of COD), 51.4 (d, ²J_{P-C} = 2.9 Hz, NCH₂), 32.4 (d, ³J_{P-C} = 2.9 Hz, CH₂ of COD), 29.4 (d, ³J_{P-C} = 2.2 Hz, CH₂ of COD), 27.2 (d, ¹J_{P-C} = 32.7 Hz, PCH₂) ppm. IR (KBr disk): ν 3107 (w), 3054 (w), 2983(w), 1579 (m), 1478 (w), 1434 (w), 1283 (m), 1178 (w), 1100 (w), 1075 (w), 1030 (w), 998 (w), 843 (w), 744 (m), 734 (s), 705 (s), 613 (s), 530 (w), 491 (m), 439 (w) cm⁻¹.

Synthesis of Cationic Iridium Complexes with Bidentate Phosphine–Pyrazolyl Ligands and Carbonyls as Co-ligands, [Ir(R₂PyP)(CO)₂]BPh₄ (R = H, Me, *i*Pr, and Ph). The synthesis of [Ir(PyP)(CO)₂]BPh₄ (**5a**)⁵⁵ is presented here with full characterization data, while the syntheses of [Ir(R₂PyP)(CO)₂]BPh₄ (R = Me, *i*Pr, **5b** and **5c**) were carried out in a similar fashion and are included in the Supporting Information.

[Ir(PyP)(CO)₂]BPh₄ (5a**).** *n*-Pentane (15 mL) (*n*-hexane can also be used) and methanol (3 mL) were added to [Ir(PyP)(COD)]BPh₄ (**3a**) (0.187 g, 0.208 mmol) under an atmosphere of nitrogen, and the suspension was degassed via three freeze–pump–thaw cycles. The reaction mixture was placed under an atmosphere of carbon monoxide for 2 h, during which time the color of the solid changed from orange to yellow. The solid product was collected by filtration, washed with *n*-pentane (4 × 3 mL), and dried under vacuum.

Yield: 0.146 g (83%). Mp: 131–133 °C (dec). ESI-MS (MeOH/dcm), *m/z* (%): ES⁺, 532.9 (15) [M – CO + MeOH]⁺, 529.1 (13) [M]⁺, 501.1 (17) [M – CO]⁺, 471.3 (100) [M – (2 × CO)]⁺; ES⁻, 319.6 (100) BPh₄⁻. ESI-MS (acetone), *m/z* (%): ES⁺, 528.5 (19) [M]⁺, 471.0 (100) [M – (2 × CO)]⁺. Anal. Found: C, 60.32; H, 4.23; N, 3.42. Calcd for C₄₃H₃₇BiRn₂O₂P: C, 60.92; H, 4.40; N, 3.30. ¹H NMR (300 MHz, CD₂Cl₂): δ 7.80 (d, ³J_{H4-H3} = 2.4 Hz, H3), 7.67–7.46 (m, 10H, CH of PPh₂), 7.35 (br m, 8H, *o*-CH of BPh₄), 6.98 (t, ³J = 7.2 Hz, 9H, *m*-CH of BPh₄ and H5), 6.39 (apparent t, ³J_{H3-H4,H5-H4} = 2.3 Hz, 1H, H4), 3.67 (m, 2H, NCH₂), 2.24 (m, 2H, PCH₂) ppm. ³¹P{¹H} NMR (121 MHz, CD₂Cl₂): δ 11.7 ppm. ¹H NMR (500 MHz, CD₂Cl₂, 200 K): δ 7.72 (s, 1H, H3), 7.62 (m, 2H, *p*-CH of PPh₂), 7.54 (m, 4H, *o* or *m*-CH of PPh₂), 7.48 (m, 5H, *m*- or *o*-CH of PPh₂ and H5), 7.32 (br s, 8H, *o*-CH of BPh₄), 6.90 (t, ³J = 7.1 Hz, 8H, *m*-CH of BPh₄), 6.78 (t, ³J = 7.1 Hz, 4H, *p*-CH of BPh₄), 6.30 (s, 1H, H4), 2.69 (m, 2H, NCH₂), 1.79 (m, 2H, PCH₂) ppm. ³¹P{¹H} NMR (202 MHz, CD₂Cl₂, 200 K): δ 11.2 ppm. ¹³C{¹H} NMR (125 MHz, CD₂Cl₂, 200 K): δ 177.4 (d, ²J_{P-C} = 104.0 Hz, CO (*trans* to P)), 170.5 (d, ²J_{P-C} = 11.2 Hz, CO (*cis* to P)), 163.5 (q, ¹J_{B-C} = 48.9 Hz, *ipso*-C of BPh₄), 148.1 (s, C3), 135.8 (s, C5), 135.2 (s, *o*-C of BPh₄), 133.1 (d, *J*_{P-C} = 11.1 Hz, *o* or *m*-C of PPh₂), 132.7 (s, *p*-C of PPh₂), 129.5 (s, *m* or *o*-C of PPh₂), 127.5 (d, ¹J_{P-C} = 60.3 Hz, *ipso*-C of PPh₂), 125.9 (s, *m*-C of BPh₄), 122.0 (s, *p*-C of BPh₄), 108.1 (s, C4), 46.9 (s, NCH₂), 24.6 (d, ¹J_{P-C} = 33.7 Hz, PCH₂) ppm. IR (KBr disk): ν 2060 (s, CO), 2024 (s, CO) cm⁻¹. IR (dcm solution, in NaCl cell): ν 2092 (s, CO), 2027 (s, CO) cm⁻¹.

[Ir(PyP)(¹³CO)₂]BPh₄ (5a'**).** The ¹³CO-enriched complex was synthesized using the same method as that used for the synthesis of [Ir(PyP)(CO)₂]BPh₄ (**5a**) using ¹³CO in place of CO. ³¹P{¹H} NMR (202 MHz, CD₂Cl₂, 298 K): δ 11.8 (br s) ppm. ¹³C{¹H} NMR (125 MHz, CD₂Cl₂, 298 K): δ 177.2 (br m, enhanced signal, ¹³CO), 171.3 (br m, enhanced signal, ¹³CO) ppm. ³¹P{¹H} NMR (202 MHz, CD₂Cl₂, 215 K): δ 11.4 (dd, ²J_{13CO(*trans* to P)-P} = 104.2 Hz, ²J_{13CO(*cis* to P)-P} = 11.2 Hz) ppm. ¹³C{¹H} NMR (125 MHz, CD₂Cl₂, 215 K): δ 177.6 (d, ²J_{P-13CO} = 104.2 Hz, ¹³CO (*trans* to P)), 170.6 (d, ²J_{P-13CO} = 11.2 Hz, ¹³CO (*cis* to P)) ppm. IR (KBr disc): ν 2043 (s, ¹³CO), 1971 (s, ¹³CO) cm⁻¹.}}}}

Synthesis of Neutral Iridium and Rhodium Complexes with Bidentate Phosphine–Pyrazolyl Ligands and Carbonyl and Chloride as Co-ligands, [M(R₂PyP)(CO)Cl] (R = H, Me, *i*Pr, and Ph, M = Ir, **6b–6d and M = Rh, **7b–7d**).** The iridium neutral complexes **6b–6d** and the rhodium neutral complexes **7b–7d** were synthesized using a method similar to that used in the synthesis of [Ir(PyP)(CO)Cl] (**6a**)⁵⁵ and [Rh(PyP)(CO)Cl] (**7a**),⁵⁵ respectively. The syntheses of **6b** and **7b** are included here, and the syntheses of **6c**, **6d** and **7c**, **7d** are included in the Supporting Information.

[Ir(Me₂PyP)(CO)Cl] (6b**).** A suspension of [Ir(μ-Cl)(COE)₂] (0.407 g, 0.454 mmol) in acetonitrile (45 mL) was degassed and placed under an atmosphere of carbon monoxide. The solid dissolved and a greenish-yellow solution of [Ir(μ-Cl)(CO)₂] was obtained after about 5 min. The reaction mixture was stirred for a further 10 min. The carbon monoxide atmosphere was replaced by an argon atmosphere, and 3,5-dimethyl-1-[2-(diphenylphosphino)ethyl]pyrazole (**2b**) (0.280 g, 0.908 mmol) in acetonitrile (10 mL) was added dropwise over 25 min. During the addition, the solution slowly turned pale yellow, and the reaction mixture was stirred for a further 45 min at room temperature. The solvent was completely removed *in vacuo*. Diethyl ether (20 mL) was added, and the pale yellow solid was collected by filtration, washed with ice cold methanol (4 × 2 mL) and *n*-pentane (3 × 5 mL), and dried under vacuum. The pale yellow solid product obtained was recrystallized by layering a dichloromethane solution (10 mL) with *n*-hexane (35 mL) and allowing it to stand at 4 °C overnight to afford [Ir(Me₂PyP)(CO)Cl] (**6b**) as a pale yellow, needle-like crystalline solid. Yield: 0.426 g (83%). Mp: 226–228 °C (dec). ESI-MS (MeOH/

Table 5. Crystallographic Data for **3b**, **6b**, **6c**, **7b**, and **7c**

| | 3b | 6b | 6c | 7b | 7c |
|---|---|---|---|---|---|
| empirical formula | C ₅₁ H ₅₃ BIrN ₂ P | C ₂₁ H ₂₃ Cl ₃ IrN ₂ OP | C ₂₄ H ₂₉ ClIrN ₂ OP | C ₂₀ H ₂₁ ClN ₂ OPRh | C ₂₄ H ₂₉ ClN ₂ OPRh |
| <i>M</i> (g mol ⁻¹) | 927.93 | 648.95 | 620.11 | 474.73 | 530.82 |
| cryst syst | monoclinic | orthorhombic | triclinic | monoclinic | Triclinic |
| space group | P2 ₁ /n(#14) | P2 ₁ 2 ₁ 2 ₁ (#19) | P1(#2) | P2 ₁ /c(#14) | P1(#2) |
| <i>a</i> (Å) | 20.923(4) | 11.2909(18) | 8.553(2) | 12.0790 | 8.590(3) |
| <i>b</i> (Å) | 9.3077(16) | 19.373(3) | 12.153(3) | 10.4534(13) | 12.219(4) |
| <i>c</i> (Å) | 22.399(4) | 20.890(3) | 12.481(4) | 16.206(2) | 12.467(4) |
| α (deg) | | | 113.091(4) | | 113.076(7) |
| β (deg) | 104.074(3) | | 90.348(4) | 102.057(2) | 90.027(4) |
| γ (deg) | | | 91.196(4) | | 91.807(5) |
| <i>V</i> (Å ³) | 4231.0(13) | 4569.3(13) | 1193.0(6) | 20011(4) | 12031.6(6) |
| <i>D_c</i> (g cm ⁻³) | 1.457 | 1.887 | 1.726 | 1.576 | 1.465 |
| <i>Z</i> | 4 | 8 | 2 | 4 | 2 |
| <i>T</i> (K) | 150(2) | 150(2) | 150(2) | 150(2) | 150(2) |
| λ Mo Kα (Å) | 0.71073 | 0.71073 | 0.71073 | 0.71073 | 0.71073 |
| μ Mo Kα (mm ⁻¹) | 3.231 | 6.280 | 5.793 | 1.08 | 0.905 |
| cryst size (mm) | 0.509 × 0.164 × 0.143 | 0.56 × 0.25 × 0.10 | 0.284 × 0.264 × 0.167 | 0.58 × 0.43 × 0.22 | 0.316 × 0.245 × 0.238 |
| cryst color | red | pale yellow | yellow | yellow | yellow |
| cryst habit | block | flat needle | prismatic | prism | block |
| <i>T</i> (Gaussian) _{min,max} | 0.309, 0.657 | 0.257, 0.749 | 0.226, 0.442 | 0.601, 0.832 | 0.766, 0.839 |
| 2θ _{max} (deg) | 56.62 | 56.04 | 56.62 | 56.04 | 56.00 |
| <i>hkl</i> range | -27 26, -12 12, -29 29 | -14 14, -25 24, -27 27 | -11 11, -15 15, -16, 16 | -15 15, -13 13, -21 21 | -11 11, -15 15, -16 16 |
| <i>N</i> | 43 524 | 43 853 | 12 012 | 18 400 | 11 481 |
| <i>N</i> _{ind} | 10 339 (<i>R</i> _{merge} 0.0447) | 10 728 (<i>R</i> _{merge} 0.0788) | 5604 (<i>R</i> _{merge} 0.0403) | 4623 (<i>R</i> _{merge} 0.0275) | 5481 (<i>R</i> _{merge} 0.0251) |
| <i>N</i> _{obs} (<i>I</i> > 2σ(<i>I</i>)) | 8858 | 9465 | 5450 | 4106 | 4892 |
| GoF (all data) | 507 | 1.028 | 1.245 | 1.064 | 1.046 |
| R1 ^a (<i>F</i> , <i>I</i> > 2σ(<i>I</i>)) | 0.0209 | 0.0351 | 0.0169 | 0.0194 | 0.0236 |
| wR2 ^b (<i>F</i> ² , all data) | 0.0475 | 0.0832 | 0.0448 | 0.0542 | 0.00653 |

^a $R1 = \sum ||F_o| - |F|| / \sum |F_o|$ for $F_o > 2\sigma(F_o)$; $wR2 = (\sum w(F_o^2 - F_c^2)^2 / \sum w(F_o^2)^2)^{1/2}$ all reflections. ^b $w = 1/[\sigma^2(F_o^2) + (XP)^2 + YP]$ where $P = (F_o + 2F_c^2)/3$; $X = 0.02$, $Y = 0$ for **3b**; $X = 0.0439$, $Y = 0.00$ for **6b**; $X = 0.02$, $Y = 0.0$ for **6c**; $X = 0.0260$, $Y = 0.8011$ for **7b**; $X = 0.03$ and $Y = 0.3$ for **7c**.

dcm), *m/z* (%): ES⁺, 560.3 (67) [M - ³⁵Cl + MeOH]⁺, 558.3 (49) [M - ³⁷Cl + MeOH]⁺, 528.7 (17) [M - Cl]⁺, 499.1 (80) [M - CO - ³⁵Cl]⁺, 497.1 (100) [MCO - ³⁷Cl]⁺. Anal. Found: C, 40.26; H, 3.88; N, 4.62. Calcd for C₂₀H₂₁ClIrN₂OP·0.5CH₂Cl₂: C, 40.60; H, 3.66; N, 4.62. ¹H NMR (500 MHz, CD₂Cl₂): δ 7.66 (br s, 4H, *o*-CH of PPh₂), 7.43–7.40 (br m, 6H, *m*- and *p*-CH of PPh₂), 5.80 (s, 1H, *H*₄), 4.84 (br, 2H, NCH₂), 2.65 (br, 2H, PCH₂), 2.52 (s, 3H, C3CH₃), 2.21 (s, 3H, C5CH₃) ppm. ³¹P{¹H} NMR (202 MHz, CD₂Cl₂): δ 13.5 ppm. ¹³C{¹H} NMR (121 MHz, CD₂Cl₂): δ 175.8 (d, ²*J*_{P-C} = 12.6 Hz, CO), 153.0 (s, C3), 142.1 (s, C5), 133.3 (br, *ipso*-C and *o*-C of PPh₂, broad resonances were observed because of fluxionality of the metal complex at room temperature), 131.3 (d, ⁴*J*_{P-C} = 2.3 Hz, *p*-C of PPh₂), 128.9 (d, ³*J*_{P-C} = 11.1 Hz, *m*-C of PPh₂), 108.2 (s, C4), 48.2 (d, ²*J*_{P-C} = 1.9 Hz, NCH₂), 30.0 (d, ¹*J*_{P-C} = 36.3 Hz, PCH₂), 15.4 (s, C3CH₃), 12.0 (s, C5CH₃) ppm. IR (KBr disk): ν 1968 (s, CO) cm⁻¹.

[Rh(Me₂PyP)(CO)Cl] (7b). 3,5-Dimethyl-1-[2-(diphenylphosphino)ethyl]pyrazole (**2b**) (0.293 g, 0.952 mmol) in methanol (20 mL) was added dropwise over 30 min to a solution of [Rh(*μ*-Cl)(CO)₂] (0.188 g, 0.483 mmol) in methanol (15 mL) under an atmosphere of argon at room temperature. A yellow-green solution with some undissolved yellow solid was obtained and the reaction mixture was stirred for a further 30 min. Approximately half of the solvent was removed under vacuum and the solid product was collected by filtration, washed with cold methanol (4 × 2 mL), *n*-hexane (3 × 3 mL) and dried *in vacuo*. The crude product was recrystallized by layering a dichloromethane (9 mL) solution of the complex with *n*-hexane (35 mL) and allowing to stand at 4 °C overnight. [Rh(Me₂PyP)(CO)Cl] (**7b**) was collected as needle-like pale yellow crystals by filtration and dried under vacuum. Yield: 0.402 g (89%). Mp. 216–218 °C (decomposed). ESI-MS (MeOH/dcm), *m/z* (%): ES⁺, 912.8 (100) [2M-Cl]⁺, 470.1 (35) [M-Cl + MeOH]⁺, 439 (100) [M-Cl]⁺. Anal. Found: C, 49.95; H, 4.52; N, 5.77. Calcd for C₂₀H₂₁ClN₂OPRh: C, 50.60; H, 4.46; N, 5.90. ¹H NMR (500 MHz, CD₂Cl₂): δ 7.67–7.63 (m, 4H, *o*-CH of PPh₂), 7.44–7.39 (m, 6H, *m* & *p*-CH of PPh₂), 5.72 (s, 1H, *H*₄), 4.83 (m,

2H, NCH₂), 2.64 (m, 2H, PCH₂), 2.45 (s, 3H, C3CH₃), 2.18 (s, 3H, C5CH₃) ppm. ³¹P{¹H} NMR (202 MHz, CD₂Cl₂): δ 41.9 (d, ¹*J*_{Rh-P} = 163.8 Hz) ppm. ¹³C{¹H} NMR (125 MHz, CD₂Cl₂): δ 189.7 (dd, ¹*J*_{Rh-CO} = 72.7 Hz, ²*J*_{P-CO} = 16.1 Hz, CO), 152.4 (s, C3), 141.8 (s, C5), 134.9 (d, ¹*J*_{P-C} = 50.5 Hz, *ipso*-C of PPh₂), 133.2 (d, ²*J*_{P-C} = 12.2 Hz, *o*-C of PPh₂), 131.2 (d, ⁴*J*_{P-C} = 2.3 Hz, *p*-C of PPh₂), 129.1 (d, ³*J*_{P-C} = 10.7 Hz, *m*-C of PPh₂), 107.8 (s, C4), 47.6 (dd, ²*J*_{P-C} = 2.3 Hz, ³*J*_{Rh-C} = 4.6 Hz, NCH₂), 30.8 (d, ¹*J*_{P-C} = 29.1 Hz, PCH₂), 15.3 (s, C3CH₃), 11.9 (s, C5CH₃) ppm. IR (KBr disk): ν 1980 (s, CO) cm⁻¹.

Crystal Structure Determination. Crystallographic details are summarized in Table 5. Single-crystal X-ray diffraction data were collected with a Bruker SMART 1000 CCD diffractometer employing graphite-monochromated Mo Kα radiation generated from a sealed tube. Data were collected at 150(2) K with ω scans to 56° 2θ, and the crystals were quenched in a cold nitrogen gas stream from an Oxford Cryosystems cryostream. The data integration and reduction were undertaken with SAINT and XPREP,⁷⁸ and subsequent computations were carried out with the WinGX⁷⁹ and XTAL⁸⁰ graphical user interfaces. In each case a Gaussian absorption correction^{78,81} was applied to the data, and there was no evidence of crystal decay.

The structures were solved with direct methods, using SIR97⁸² or SHELXS-97, and extended and refined with SHELXL-97.⁸³ The

(78) SAINT and XPREP; Bruker Analytical X-ray Instrument Inc.: Madison, WI, 1995.

(79) Farrugia, L. J. *J. Appl. Crystallogr.* **1999**, *32*, 837–838.

(80) Hall, S. R., du Boulay, D. J., Olthof-Hazelkamp, R., Eds. *Xtal3.6 System*; University of Western Australia: Perth, Australia, 1999.

(81) Coppens, P.; Leiserowitz, L.; Rabinovich, D. *Acta Crystallogr.* **1965**, *18*, 1035–1038.

(82) Altomare, A.; Burla, M. C.; Camalli, M.; Cascarano, G. L.; Giacovazzo, C.; Guagliardi, A.; Moliterni, A. G. G.; Polidori, G.; J., S. R. *J. Appl. Crystallogr.* **1998**, *32*, 115–119.

(83) Sheldrick, G. M. *SHELXL-97*; Institut für Anorganische Chemie der Universität, University of Göttingen: Tammanstrasse 4, D-3400 Göttingen, Germany, 1998.

non-hydrogen atoms were modeled with anisotropic displacement parameters, and a riding atom model with group displacement parameters was used for the hydrogen atoms. ORTEP⁸⁴ depictions are provided in Figures 1, 4, and 5, with displacement ellipsoids shown at the 50% level except for complex **3b**, for which the ellipsoids are shown at 20%. Complex **6b** crystallized in the non-centrosymmetric space group $P2_12_12_1$ (#19), and the absolute structure was determined with the Flack parameter^{85–88} refining to 0.000(6).

(84) Johnson, C. R. *ORTEP*; Oak Ridge National Laboratory: Oak Ridge, TN, 1976.

(85) Flack, H. D. *Acta Crystallogr. Sect. A* **1983**, *39*, 876–881.

(86) Bernardinelli, G.; Flack, H. D. *Acta Crystallogr. Sect. A* **1985**, *41*, 500–511.

(87) Flack, H. D.; Bernardinelli, G. *Acta Crystallogr. Sect. A* **1999**, *55*, 908–915.

(88) Flack, H. D.; Bernardinelli, G. *J. Appl. Crystallogr.* **2000**, *33*, 1143–1148.

Acknowledgment. Financial support from the Australian Resereach Council is gratefully acknowledged. K.Q.V. would like to thank the government of Australia for an Endeavour International Postgraduate Research Scholarship and the School of Chemistry for a Postgraduate Teaching Fellowship. We would like to thank Dr. Russ Pickford and Dr. Keith Fisher for obtaining ESI-MS and Susanne L. Huth for assistance with crystallographic work.

Supporting Information Available: Full experimental details for the synthesis of compounds 3,5-diisopropylpyrazole, 1,2-bis-(3,5-dimethylpyrazol-1-yl)ethane, 1,2-bis(3,5-diisopropylpyrazol-1-yl)ethane, **2c**, **2d**, **3b–3d**, **4a–4d**, **5b**, **5c**, **6c**, **6d**, **7c**, **7d**, and **7c'**, **7d'**; time course data for the catalyzed cyclization of **8** with complexes **3a–3d**; CIF files for complexes **3b**, **6b**, **6c**, and **7b**, **7c**. This material is available free of charge via the Internet at <http://pubs.acs.org>.

OM070057V